Build Simul (2023) 16: 1691–1712
https://doi.org/10.1007/s12273-022-0940-x

Numerical evaluation of enhanced green infrastructures for mitigating urban heat in a desert urban setting

Afifa Mohammed[1] (✉), Ansar Khan[2], Mattheos Santamouris[1]

1. Faculty of Built Environment, University of New South Wales, Sydney, Australia
2. Department of Geography, Lalbaba College, University of Calcutta, Kolkata, India

Abstract

The cities of desert climates are anticipated to recognize a synergy of urban heat island (UHI) and severe heat waves during summertime. To improve the urban thermal environment, the present study aims quantitatively explore a strategically designed network of vegetation patches called green infrastructure (GI) in subtropical desert cities such as Dubai. To achieve a more comfortable temperature environment, we built and simulated four GI situations with higher GI fractions, GI25, GI50, GI75, and GI100. Using a mesoscale urban model, the mosaic approach is utilized to test potential thermal improvement and urban climate impact, and a portion of each urban grid cell in the model domain is altered with various species of urban vegetation patches by 25%, 50%, 75%, and 100%. The daily peak reduction in ambient temperature at 17:00LT is similar to 0.0168 °C per unit of GI increase when compared to the untreated scenario; however, the maximum anticipated daytime summer temperature decline for GI25, GI50, GI75, and GI100 is 0.6 °C, 1.1 °C, 1.4 °C, and 1.7 °C, respectively. The associated reduction in nighttime ambient temperature per unit increase in the GI is 0.0432 °C, with a maximum temperature drop of around 2.4 °C for the GI100 scenario. Increased GI reduces the height of the planetary boundary layer (PBL) by up to 468 m, which might lead to greater pollution concentrations. While GI-based cooling has a significant influence on delayed sea breeze and humidity, it may raise the risk of heat discomfort in the indoor building environment. This study adds to our understanding of the potential for GI mitigation as well as the seasonal impact of developing GIs on the desert urban boundary layer.

Keywords

green infrastructure;
heat mitigation;
urban heat;
WRF-SLUCM;
Dubai city

Article History

Received: 03 July 2022
Revised: 15 August 2022
Accepted: 07 September 2022

1 Introduction

Climate change and growing urbanization offer substantial environmental challenges, and they are among the key issues that governments, scientists, and planners face across the world. The building materials used on urban impermeable surfaces generate greater runoff and lower water infiltration, as well as higher thermal conductivities, which inhibit evapotranspiration in plant cover and enhance solar radiation absorption. Several studies have shown that the amplitude of urban heating rises dramatically during heatwaves owing to local climatic synergy (Founda and Santamouris 2017). Extreme urban heat can have a massive impact on the environment, including irrigation water demand for vegetation areas, energy demand for cooling systems, excess electricity demand, the doming effect of urban pollutants, human biometeorology, and heat-induced mortality and morbidity, particularly for low-income households (Yu and Hien 2006; Santamouris 2020). Temperature rises of up to 10 °C have been experimentally confirmed in over 450 cities, with a typical value of 5 °C (Santamouris 2015a, b).

Numerous studies suggest that urban heating harms the human thermoregulatory system, significantly increasing heat-related illness and death (Johnson et al. 2004). According to climate change forecasts, heatwave dangers will escalate in the future as heatwave intensity, frequency, and duration increase (Cowan et al. 2014). High ambient temperatures in cities promote photochemical processes in the lower atmosphere, reducing urban air quality. Ground-level ozone, a pollutant that is very harmful to people, is produced as

E-mail: a.mohammed@student.unsw.edu.au

a result of the interaction between ambient NOx and hydrocarbons (Pyrgou et al. 2018). According to studies, between 2013 and 2015, the ozone concentration in 75 Chinese cities grew from 69 to 75 parts per billion, while the entitlement of non-compliant cities increased from 23% to 39% (Wang et al. 2013).

Cities' urban heating has a considerable influence on ground-level ozone concentrations (Stathopoulou et al. 2008; Wang et al. 2013). According to several kinds of research, the frequency of possible ozone events in four major Canadian cities with distinct synoptic weather patterns is expected to rise by 50% by 2050 and by 80% by 2080 (Jacob and Winner 2009; Wise 2009). Several studies have looked into the efficacy of developing and implementing various mitigation technologies and strategies, such as reflective materials in buildings, the use of water bodies, increasing green infrastructure (GI) in cities, solar control and shading devices, utilizing evaporative systems, and changing the geometry of urban infrastructure to counteract the effects of urban heat (Santamouris et al. 2011; Middel et al. 2014; Santamouris 2014; Akbari et al. 2015; Gao et al. 2020; Santamouris and Osmond 2020; Santamouris and Yun 2020). Numerous experimental evaluations and theoretical analyses of urban heat mitigation studies have shown that existing technologies or strategies could decrease the ambient temperature by up to 3 °C, lowering cooling demand, electricity use, and heat-related morbidity and mortality (Santamouris 2014; Santamouris et al. 2017; Haddad et al. 2020; Santamouris et al. 2020; Khan et al. 2022a).

As cities expand, they face a variety of challenges that highlight the need to improve urban sustainability and resilience by integrating social, technological, and ecological systems centered on the establishment of a network of natural and planted vegetation, such as street trees, cool roofs, rain gardens, community gardens, wetlands, and green walls (Akbari et al. 2001; Foster et al. 2011; Kolokotsa et al. 2018; Andersson et al. 2019). It has been discovered that GI is the main technique for doing this. Several definitions of GI differ in focus and scale. Many ecologists see GI as a multi-scale network of ecological components that delivers a variety of functions and benefits (Benedict and McMahon 2002). According to the European Environmental Agency, GI is a network of green features that are integrated to give additional advantages and resilience (European Environmental Agency 2011). While another study defines GI as "a network of natural and semi-natural green spaces such as forests, parks, green roofs and walls that can provide nature-based and cost-effective solutions" (Connop et al. 2016), it is measured as vegetation or vegetated spaces that offer numerous ecosystem services in Canada (Conway 2020). In the United States (US), green stormwater infrastructure is largely positioned as an on-site storage and infiltration solution to stormwater management, even though it is projected to provide environmental, social, and economic advantages (McPhillips and Matsler 2018; Spahr 2020). In addition to storing stormwater runoff, carbon sequestration, and promoting human health in metropolitan areas, urban greenery plays a critical role in lowering urban overheating and eliminating pollutants (Santamouris et al. 2018).

The presence of urban vegetation and evapotranspiration decreases the impact of heatwaves by changing the energy balance of the city's surface and lowering heat storage on urban surfaces (Loughner et al. 2012; Jacob et al. 2018). Based on an analysis of fifty-five case studies on urban heating, extreme urban heat-induced mortality, and environmental quality, a statistically significant correlation between the increase of urban GI in the daytime and nighttime peak ambient temperatures was discovered; additionally, urban vegetation increases night-time cooling by reducing heat storage on the city's surface through direct shading (Santamouris and Osmond 2020). The shade supplied by the tree canopy was the most important element influencing the ambient temperature in the vegetation, while tree attributes and shape played a small influence (Shashua-Bar and Hoffman 2000). The greenery in urban areas considerably helps the improvement of human thermal comfort. Using a Princeton urban canopy model (PUCM) linked with the weather research and forecasting (WRF) model, a study in Melbourne investigated the efficiency of adding green spaces, cooling roofs, or combining both to alleviate human temperature stress in urban settings. It was found that the proportion of urban grass was increased to test the efficacy of urban vegetation in lowering urban temperatures (Coutts et al. 2016; Jacobs et al. 2018). Increasing GI in urban areas leads to a reduction in heat-related mortality since a 1 °C drop in temperature reduces heat-related mortality by 3% on average (Santamouris and Osmond 2020). Several studies have demonstrated the importance of mixed forests, shrublands, and grasslands in lowering urban heat when introduced as part of GI (Imran et al. 2019). There are several discoveries addressing the advantages of GI that necessitate in-depth research for climatic zones and urban settings, where combining a building science approach with vegetation scenarios is critical and urban areas necessitate the spread out of plantations and public gardens (Chatzinikolaou et al. 2018; Givoni 1989).

In hot and dry locations, the study found that planting trees in low-density areas can lower the temperature by 2 °C in Baghdad (Abaas 2020). Furthermore, in Cairo, half of the trees are successful in reducing power consumption and air temperature by 0.2–0.4 °C in high-density built-up regions, but inefficient in low-density built-up areas (Aboelata and Sodoudi 2020). In Dubai, it has been demonstrated that some plants may reduce pollution and enhance air

quality by filtering out dust acquired from a landscaping buffer around an urban population, in addition to temperature decreases (Taleb 2016). According to the Environment Agency of Abu Dhabi, the temperature in various locations of the UAE is rising significantly owing to rising levels of greenhouse gas emissions, which influence the microclimate of metropolitan cities, the built environment, and the economy (Radhi 2010). As a result, the Abu Dhabi Department of Municipalities and Transport (DMT) has issued a Public Realm Design Manual that includes a list of local climate-sensitive tree species as the first step toward mitigation (Abu Dhabi Department of Planning and Municipalities 2010). In contrast, the Manual lacks scientific grounds for the impacts of vegetation scenarios on air temperature (Abu Ali and Khanal 2021). According to the findings of Abu Dhabi research, certain urban trees can reduce temperatures by 0.9 °C when putting every six meters in paths and unshaded areas (Abu Ali and Khanal 2021).

There have been many studies on the use of urban green infrastructures as heat mitigation strategies (Gunawardena et al. 2017; Lai et al. 2019; Wong et al. 2021; Aram et al. 2019; Fu et al. 2022). Given the vast amount of study in the literature have been conducted to assess the efficacy of changed urban GI components on urban climate and cooling potential under current and future urban growth, there is still much ambiguity surrounding cooling capacity and its impact on subtropical desert urban climate. Under normal climatic conditions, a desert urban setting may only support a limited quantity of vegetation; vegetations are frequently missing, and shrubs or herbaceous plants offer insufficient ground cover. These ambiguities in terms of expected GI fraction and temperature drop. The existing literature has a wealth of facts and information. However, because of the large variety of research topics covered and methodology used by each study, the spectrum of supplied questions, results, and conclusions is very broad, and in some cases contradictory even within the same city. As a result, it is a huge source of consternation, potentially worsening urban climatic, environmental, and health issues. Given that the majority of cooling demand occurs during the day, shifting the greatest mitigation potential of trees to the night diminishes the predicted cooling contribution. Potential difficulties of night warming and significant increases in humidity levels recorded by several studies should not be overlooked, especially when extra trees are deployed in urban canyons, limiting the sky view factor, and increased GI is planned in humid countries. For comparison purposes, forty-six large-scale GI-based researches were included in this study to explore the impact of increasing GI fraction in thirty cities. The locations and localities of each research were thoroughly reviewed and statistically reported. For scientific approval, the data from these cities were extensively analyzed and quantitatively compared to current data. However, relatively few studies have described the biophysical consequences of the GI on the surface standard meteorological field and planetary boundary layer (PBL) that are caused by seasonal fluctuations in the GI. In addition, there is a lack of data and understanding about the benefits and drawbacks of GI policies, as well as the consequent cost to contribute to the decision-making process in greenery plans. Attributable to severe aridity, many deserts are almost devoid of flora; nonetheless, this study is assumed to be due in part to the impacts of extra particular vegetation species on leafy urban environments and seasonal temperature benefits to escape the urban heat.

The goal of this study is to numerically evaluate the effectiveness of limited, average, and high-level increases in urban GI on urban cooling potential and regional urban climate in Dubai in terms of sensible and latent heat flux, air and surface temperature, relative humidity, wind speed, and PBL by designing and assessing four mitigation potential scenarios associated with increased GI using advanced mesoscale urban modeling. The studies found the seasonal effects of climatic variable fluctuations caused by changes in urban vegetation conditions. The application of GI-based urban cooling to lower PBL heights is very exciting. The study's findings have implications for improving urban vegetation management in dry areas like Dubai.

2 Background

Dubai is located on the Tropic of Cancer, bounded by 25°16' N and 55°18' E. The city has a 72-km long coastline on the Arabian Peninsula's eastern shore and faces the Arabian Gulf to the southwest (Al-Sallal and Al-Rais 2012). Dubai has rapidly urbanized and has become one of the world's most notable urbanizing cities in a very short period. With an area of 4114 km^2, the city accounts for 5% of the UAE's total territory, making it the country's second-largest metropolis among the seven emirates. In recent decades, significant urban developments have led to Dubai's fast population increase and urban climate alteration. According to the Statistics Centre of Dubai, UAE, it reached 3.41 million by the end of 2020, a rise of 55,300 over the previous year, and a growth rate of 1.63%.

Due to its geographical position, Dubai's climate is subtropical and desert, with hot and humid summers and mild winters. The ambient temperature rises to 48 °C in the summer and falls to between 10 °C and 30 °C in the winter (Al-Sallal and Al-Rais 2012). From May 19th to September 24th, average daily temperatures surpass 37 °C for 4.1 months, with August being the warmest month of the year with an average high of 40 °C and a low of 31 °C. While the chilly season lasts 3.1 months, with average daily temperatures

below 27 °C from December 5 to March 9, January is the coldest month of the year, with an average low of 15 °C and a high of 24 °C (weatherspark 2022). Dubai's urban heating is mostly influenced by synoptic weather conditions (i.e., sea wind and warm air advection from the desert fetch) and is greatest at night. Extreme urban temperature occurrences will become more regular and prolonged in coastal cities such as Dubai. Figure 1 depicts the hourly temperature trend in Dubai (1980–2020). Since the 1990s, the magnitude of urban temperature has increased alarmingly. The statistics suggest a 0.77 °C average increase since 1980. These occurrences have resulted in a persistent temperature issues and human discomfort during the summer. The ambient temperature and night-time UHI intensity are 1.3 °C and 3.3 °C higher in the core urban region, respectively than in the immediate rural environs, and the UHI and ambient temperature are independent of each other only when the wind originates from the desert. According to a recent study (Mohammed et al. 2020), there is a negative and inverse relationship between urban heating and wind speed. According to the findings of this study, the degree and amplitude of urban heating are strongly related to local meteorological conditions and changes in local convection over the immediate land surface.

In recent years, the UAE has taken urgent action to prevent and adapt to the effects of urban climate change, putting out a long-term climate and energy policy route and measures. In 2017, the government took action on climate change by enacting the National Climate Change Plan 2017-2050, which establishes a framework for controlling greenhouse gas emissions, climate change adaptation, and private-economic sector innovations.

The urban climate in Dubai is influenced by the conversion of land use and vegetation cover. The major native plants of the UAE are *Cornulacamonacantha*, *Desert Hyacinth (Cistanchetubulosa)*, *Arta (Calligonumcomosum)*, *Date Palm – Nakhl*, *Nakheel*, *Nakhla*, *Arfaj (Rhanteriumepapposum)*, *Ausaj (Lyciumshawii)*, *Safrawi (Dipterygium glaucum)*, *and Shuntop (Pentatropis nivalis)*. The government of Dubai emphasizes the importance of GIs (urban green, nature conservation reserves, and farms) that are invaluable and have a significant impact on reducing urban heat in urban areas, which supports the Dubai 2040 Master Plan to expand vegetation areas in the city (Figure 2). Increasing vegetation spaces can alter the surface energy balance by decreasing stored heat in urban surfaces and increasing evapotranspiration (Loughner 2012), which converts net radiation into latent heat. Furthermore, urban vegetation may immediately shade the urban surface, reducing storing heat and so improving nighttime cooling.

The size and spacing of green areas are critical for the surrounding areas to benefit from the optimal cooling influence. Greenery has been increased in the city, particularly on all roads and residential areas, where the greening plan for Dubai municipality presents that the vegetation area for each of Dubai's residents is around 13.25 to 25 m^2 in 2020 (Bolleter 2014). Furthermore, green space coverage increased to roughly 43,830 m^2 by planting more than 170,000 trees in 2021, with a daily average of 466 trees planted. Several tree species were planted along external highways to minimize sand invasion, as well as local species that can help alleviate the impacts of climate change in open desert areas and soil erosion. New trees, such as Al Busida and Green Cassia, have also been planted to withstand the environment. Artificial

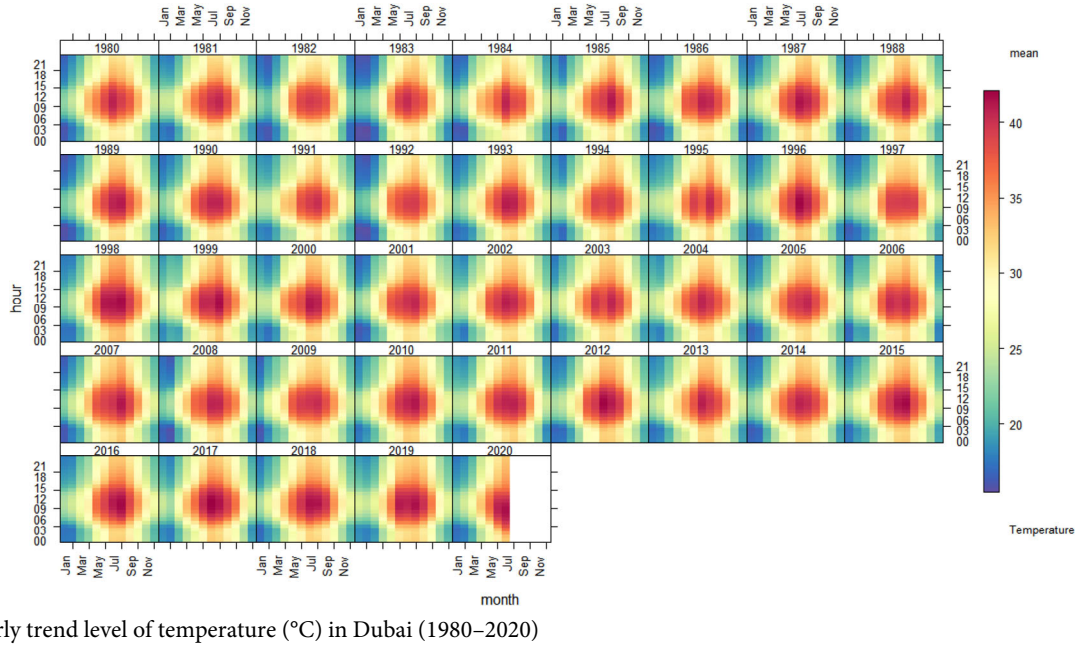

Fig. 1 Hourly trend level of temperature (°C) in Dubai (1980–2020)

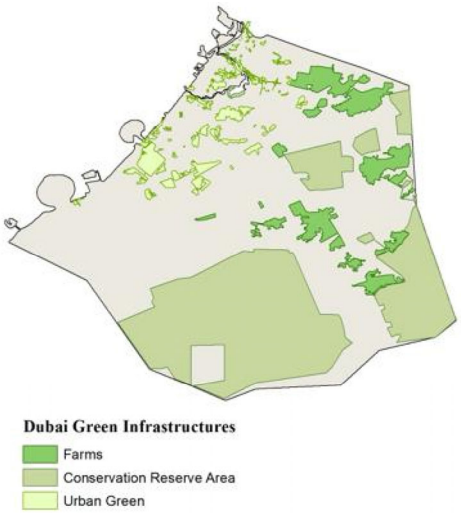

Fig. 2 The existing green infrastructure mainly comprises farms, reserve area, and urban green

intelligence has been used to improve irrigation system efficiency and the city's urban sustainability.

The GI in Dubai considerably helps to decrease land surface temperatures by increasing and balancing plant cover, which can aid in managing the local climate and moderating the urban heat impact. The shaded green spaces with palms, park trees, flowering trees, seasonal plantings, and other species were adapted to the area's severe temperatures and offer an appealing oasis of green to service the zone and roadways such as those in the downtown area. Because of the region's climate change influence, the buildings and surrounding GI may synergize remarkably well. For example, the hot and humid environment combined with Tower Park's chilled water-cooling system generates substantial amounts of condensation, with around 15 million gallons collected and used in the irrigation system each year. Another section is the Expo 2020 site, which spans 4.38 km. It includes a 220 km^2 nursery with over 12,157 trees and palm trees, more than 256,000 bushes, and hundreds of flowering plants and herbs, all employing sustainable technology such as solar electricity.

Nature reserve areas in Dubai are part of the environmental, sustainability, and tourist sectors, and they also provide scientists and researchers with a field study opportunity. There are 8 nature reserves in Dubai, covering 16.5% of the city's area, including the mountainous Hatta reserves (28.08 km^2), the desert Marmoum reserves (361.9 km^2), the desert monsters reserves (15.06 km^2), the Dubai desert (Al Maha) reserves (226 km^2), which covers nearly 5% of the total land of Dubai, as well as Jebel Nizwa (1.06 km^2) and Ghaf Nizwa (0.128 km^2) to be (76.67 km^2). These natural reserves are home to a diverse range of animals and birds, as well as several native florae such as Ghaf, Samar, Sidr, Miswak, Ashkhar, and Ramram trees, bitter melon, meadows, and acacia trees. Furthermore, at the Jebel Ali Wildlife Sanctuary in Dubai, the first mangrove forest was planted, which is regarded as the most ecologically favorable tree kind. It is distinguished by its minimal water use in irrigation owing to surviving on saltwater, as well as its capacity to isolate carbon at a rate of 3 to 5 times that of other types of forest trees. On this front, Dubai urban plan 2040 anticipates that 60% of the regions will be natural reserves.

3 Materials and methods

The general background of the current investigation is global warming and excessive urban heat. Because the materials used in building and urban fabrics influence urban thermal balance and contribute considerably to excessive urban heat, major efforts have been made to incorporate nature-based solutions such as GI that present low surface temperatures in the outer environment. The GI offers significant cooling potential for extreme urban management in cities. As a result, utilizing the mesoscale urban model as a holistic and dynamic analytical tool, the benefits and downsides of adopting GIs for subtropical desert climates as an example of Dubai city have been delimited for the first time in terms of environmental and meteorological repercussions.

3.1 WRF model configuration

The community WRF (v4.3.3) was employed in conjunction with a highly advanced single-layer urban canopy model (SLUCM) to assess the efficacy of GI for urban thermal management (Chen and Dudhia 2001; Kusaka et al. 2001; Skamarock et al. 2008; Qi et al. 2021). The WRF coupled with the SLUCM is configured over a parent domain and two nested domains cantered in Dubai city (25°16 N and 55°18' E), with spatial resolutions of 18 km, 6 km, and 2 km for d01, d02, and d03, respectively. The Dubai city area is focused on the innermost domain (d03), which has a spatial resolution of 2 km and includes the whole city (Figure 3). Table 1 details the physics parameterization of the model used in the current numerical evaluation of GI. The meteorology of the WRF-initial and boundary conditions was driven by ERA-Interim reanalysis data. The ERA-Interim is a worldwide atmospheric reanalysis that runs from January 1, 1979 to August 31, 2019 (https://www.ecmwf.int/en/forecasts/datasets/reanalysis-datasets/era-interim). The ERA5 reanalysis has surpassed it. The data assimilation method used to create ERA-Interim is based on an IFS release from 2006. (Cy31r2). A 4-dimensional variational analysis (4D-Var) with a 12-hour analysis window is included in the system. The data collection has a spatial resolution of around 80 km (T255 spectral) on 60 levels in the vertical from the surface

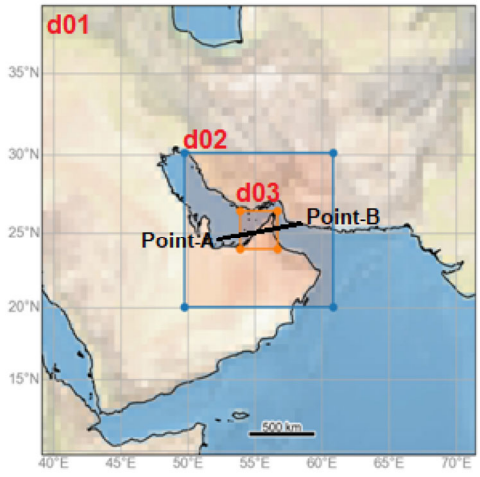

Fig. 3 WRF domain shows (a) dynamical downscaling with domain 1 (d01) as the outermost parent domain with 18 km grid spacing, domain 2 (d02) with 6 km grid spacing, and, an innermost domain 3 (d03) with 2 km grid spacing; (b) innermost d03 with 2 km grid spacing which encompasses the Dubai city. Point-A (left) and Point-B (right) are the points used for drawing horizontal-vertical cross-sections to analyze meteorological conditions for Fig. 12

Table 1 WRF/SLUCM Model configuration

Configuration	Domain 01 (d01)	Domain 02 (d02)	Domain 03 (d03)
Version	ARW-WRF v4.3.3		
Initial and boundary conditions	ERA-Interim reanalysis data (0.75° × 0.75°)		
Run time			
Time period for analysis	July 2019 and January 2019		
Grid distance (km)	30	6	2
Grid number	120 × 120	206 × 206	154 × 154
Number of vertical layers	33 layers		
Microphysics	Thompson graupel scheme (Thompson et al. 2008)		
Surface layer model	Noah-LSM+Single layer UCM (Chen and Dudhia 2001; Kusaka et al. 2001)		
Turbulence	Mellor and Yamada's (1974) TKE scheme		
Short-wave radiation	RRTMG scheme (Iacono et al. 2008)		
Long-wave radiation	RRTMG scheme (Iacono et al. 2008)		
Planetary boundary layer	Mellor-Yamada-Janjic (Eta) TKE scheme (Janjić1994)		
Cumulus parameterization	Tiedtke scheme (Tiedtke 1989; Zhang et al. 2011)		

to 0.1 hPa. To simulate the actual urban climate in the Dubai area, dependable land use and land cover (LULC) data that constrain rapid urban expansion are necessary. The LULC distribution was classified using a 2019 Landsat image with a spatial resolution of 30 m. The Landsat image was classified in the ArcGIS environment using the support vector machine (SVM) method. We focused on three forms of land use to keep things simple: built-up land (urban), water bodies, and other geographies. Further urban built-up lands (urban) are classified into three types: industrial/commercial, high-density residential and low-density residential. Low-density residential areas have population less than 500 person per km^2 and anthropogenic heat (AH) less than 10 W m^{-2}, whereas industrial/commercial areas have population higher than 1000 person per km^2 and AH greater than 40 W m^{-2}. The remaining areas are classified as high-density residential regions. The classified LULC map was then overlaid in domain 3 (d03) on the WRF model's default USGS LULC database. The USGS's LULC dataset includes urban and built-up land as the urban-type, with the following three categories providing more detailed classifications of urban land use type: low-density residential, high-density residential, and industrial or commercial. We utilized WRF with urban physics enabled (sf urban physics! = 0 for d03), and the three categories of urban built-up lands are intended to more accurately depict urban features (Khan et al. 2022b). Although the USGS LULC schemes for urban and built-up terrain do not include AH, it does have a value that corresponds to low-density residential, high-density residential, and industrial or commercial. The improved LULC is then used in conjunction well with the WRF pre-processor to assign values to each urban grid cell. The Noah-LSM and SLUCM are designed to account for the large LULC data in the urban domain. During the summer and winter months of the considered period, the sky was clear and the breezes were gentle. The efficacy of GI heat reduction measures was evaluated using hourly simulation data over the innermost area (d03). The first 72 hours of the control and modified GI simulations were treated as WRF model spin-up time and were thus excluded from the research's subsequent analysis.

3.2 Numerical design for mesoscale green infrastructure

The GI strategies are a viable approach to reducing urban heat. Additional GI has a significant influence on the energy balance components of the urban surface (solar radiation, sensible heat, latent heat, advection, and heat storage). It can also have an impact on city-scale thermodynamics by altering moisture exchange and availability on the urban surface as well as in the lower atmosphere. However, actual data on the optimal GI approach for increasing human thermal comfort in cities is still lacking. In addition, Dubai lags behind cities in the United States, Europe, and Oceania in terms of using GI to reduce urban heat. As a result, this work hypothetically designed the expanding GI for Dubai, UAE, employing the WRF-SLUCM to minimize urban heat and its climatic implications via vegetated patches comprised of varied vegetation types.

In Noah LSM, LULC in urban climate research may be regulated by either dominating land-use categories (existing LULC) or a mosaic approach (user option). The dominant land-use type refers to the entire urban grid cell, which corresponds to a single LULC category; however, the mosaic technique pass on an urban grid cell can be sub-gridded into several tiles, reflecting many LULC categories inside a single urban grid cell (Sharma et al. 2017; Imran et al. 2019; Khan et al. 2022). Mosaic makes advantage of the intra-grid dispersion of each land-use group. If the LULC resolution is higher than the grid resolution, we may have profited from the mosaic technique. The changes have to be made to the land use fractions in the WRF geogrid file. Then, depending on the user's preferences, we may employ different LULC and their fractions in each grid cell. It must also update the geogrid file's landmask variable. This method is suitable for investigating the impacts of greening up large parts of metropolitan grid cells. To quantify the performance of various types of GI, a section of each urban grid cell is replaced with supposed plant patches, particularly GI25, GI50, GI75, and GI100, using the mosaic technique (vegetation patches). Vegetation patches as GI in this study are a combination of several forms of urban greenery, which supports the Dubai 2040 Master Plan's aim of developing vegetation areas throughout the city. For future urban climate control, the Dubai government highlights the need for GIs such as urban green, natural conservation zones, and farms. As a result, the current study quantified the urban climatic advantages of evergreen forests, deciduous forests, shrubs, and grasslands at the city scale. As shown in Table 2, simulations of vegetation patches were performed by varying the land-use proportion inside mosaic urban grid cells by final GI, such as 25%, 50%, 75%, and 100%. Table 3 highlights the input parameters for the many vegetation types that may be encountered.

In veracity, such a high proportion of GI in metropolitan areas is unsustainable in a realistic scenario. It is well recognized that turning all open space in an urban zone into urban green space will fall short of the World Health Organization's (WHO) goal of 50% green space. The maximal cooling capacities of urban greenery, as well as the influence of increased urban greenery on urban climate, are of great scientific interest. In the subtropical desert climate of the Dubai metropolis, four modified GI scenarios with an increasing rate of the beginning GI value of 0.10 (control case) to 0.15, 0.40, 0.65, and 0.90 were investigated in Table 2. This explicitly refers to the initial GI value is 0.10, with increments of 0.15 (0.10 + 0.15 = GI25), 0.40 (0.10 + 0.40 = GI50), 0.65 (0.10 + 0.65 = GI75), and 0.90 (0.10 + 0.90 = GI100). This entails one control scenario (GI10) and four modified GI scenarios (GI25, GI50, GI75, and GI100). When widely available urban greens are

Table 2 Numerical design for the heat mitigation study

	Mitigation strategies		
Scenario	Urban fraction (%)	Vegetation patches (%)	Land use fraction modification with Mosaic approach
Control case (CTRL)	90%	10%	90% Urban and built-up land + 10% default vegetation
Green infrastructure 25% (GI25)	75%	25%	75% Urban and built-up land + 10% Deciduous broadleaf forest + 10% Deciduous needle leaf forest + 5% Shrub land
Green infrastructure 50% (GI50)	50%	50%	50% Urban and built-up land + 20% Deciduous broadleaf forest + 20% Evergreen broadleaf forest + 10% Grassland
Green infrastructure 75% (GI75)	25%	75%	25% Urban and built-up land + 20% Evergreen broadleaf forest + 25% Evergreen needleleaf forest + 10% Deciduous broadleaf forest + 10% Deciduous needle leaf forest + 5% Shrub land + 5% Grassland
Green infrastructure 100% (GI100)	0%	100%	0% Urban and built-up land + 30% Evergreen broadleaf forest + 30% Evergreen needleleaf forest + 15% Deciduous broadleaf forest + 15% Deciduous needle leaf forest + 5% Shrub land + 5% Grassland

Table 3 Different default key properties of urban area and vegetated parameters (USGS) in the WRF model

Properties	Shade factor factor	Minimum LAI	Maximum LAI	Minimum Albedo	Maximum albedo
Urban	0.10	1.00	1.00	0.15	0.15
Deciduous broadleaf forest	0.80	2.80	5.50	0.17	0.25
Deciduous needle leaf forest	0.70	1.00	5.16	0.14	0.15
Evergreen broadleaf forest	0.95	3.08	6.48	0.12	0.12
Evergreen needleleaf forest	0.70	5.00	6.40	0.12	0.12
Shrub land	0.70	0.50	3.66	0.25	0.30
Grasslands	0.80	0.52	2.90	0.19	0.23

employed at the city scale, a GI fraction of 0.15 to 0.60 may be achieved, proving the concept in practice. The third scenario provides for a greater GI proportion at the furthest limit of GI-based urban cooling. Given the rapid advancement of planning science, which yields values of more than 0.70 for newly built urban areas in developed countries, it is imperative to examine the cooling ability and impact of these GI values at the urban scale for the desert environment. These assumptions GI scenarios can provide urban planners, urban climatologists, and legislators with a transcendental grasp of urban heat mitigation, allowing them to design and execute urban green space solutions in next-generation smart cities.

3.3 Model validation and evaluation

Following on from our previous study, in which we tested and evaluated the performance of cool materials in Dubai city (Mohammed et al. 2021), we analyzed the entire months of January 2019 and July 2019. The United Arab Emirates (UAE) National Centre of Meteorology (NCM) provides hourly ambient temperature data based on different in-situ meteorological observations. We employed four local meteorological data sets from distinct urban LULC settings that are kept by the NCM and used for WRF model validation and assessment in this study. To test and analyze the WRF model performance, the hourly output of 2 m temperature at the seasonal scale (summer and winter) from the untreated simulation (control scenario) was statistically compared with separate local meteorological observations. Moreover, each observation is confined within the inner domain (d03) of the model with a fully underlying urban grid cell in nature. The values of each statistical measure such as correlation coefficient (r), mean absolute error (MAE), root mean square error (RMSE), and mean bias error of hourly ambient temperature for six local observations with a control run of the WRF model were estimated and summarized in Table 4. All statistical measures were highly corroborated with the WRF model to control case for six meteorological observations. For correlation, the WRF model was highly twisted with all local observations for the summer months (0.84 to 0.89) and winter months (0.82 to 0.89). The range of MBE air temperature is varied from −0.2 °C to 1.06 °C for the summer months and 1.58 °C to 2.68 °C for the winter month. These mean biases in the model bear out that no necessary steps need to be taken to correct the model bias. The ambient temperature value of RMSE is varied from 2.53 °C to 2.93 °C for a summer month and 2.03 °C to 2.95 °C for a winter month, which divulge that the model temperature is in the region of the line of best fit is determined. The index of agreement (IOA) also demonstrates excellent accord for the seasonal scale is 0.92 for summer months and 0.76 for winter months, respectively. The control simulation is well twisted with the surface standard meteorological field and statistically granted with local meteorological observations at a significant probability level ($p \leq 0.05$). The validation results have confirmed that the control run of the WRF model is successfully replicating the actual urban climatic condition for subsequent exploring the performance of the GI mitigation strategy.

Table 4 Comparison of the simulation results with observation 2-m air temperature data during summer and winter month (Mohammed et al. 2021). The weather stations used by the authors collect data at elevations ranging from 19 to 138 m above ground level. To validate the model's performance, we used the hypsometric equation to interpolate at 2-m level (Guinn and Mosher 2015). Because the heights of the stations ranged from 19 to 138 m, this does not appear to have a significant influence. Even a 6.5 °C km^{-1} will only change the temperature by around 0.65 °C, but the bias in WRF will be on the order of 2 °C or more. Although dubious, the Monin-Obukhov similarity theory's above-roof air temperature is often used to analyze the efficacy of SLUCM (e.g., Li and Bou-Zeid 2014)

Parameters	Weather station			
	A	B	C	D
	Summer			
Correlation coefficient	0.89	0.86	0.84	0.84
Mean bias error	−0.22	0.05	1.06	0.89
Mean absolute error	−0.22	0.05	1.06	0.88
Root mean square error	2.54	2.93	2.53	2.69
Index of agreement	0.95	0.93	0.89	0.90
	Winter			
Correlation coefficient	0.85	0.82	0.89	0.83
Mean bias error	1.72	2.68	1.69	1.58
Mean absolute error	1.72	2.68	1.69	1.58
Root mean square error	2.04	2.95	2.23	2.03
Index of agreement	0.68	0.78	0.85	0.73

Note: A= Dubai International Airport Station (latitude: 25°15'10", longitude: 55°21'52", elevation: 19 m, landuse: urban, population density = 3611 person km^{-2}), B = Al-Maktoum International Airport station (latitude: 24°55'06", longitude: 55°10'32", elevation: 52 m, landuse: suburban, population density = 825 person km^{-2}), C = Saih Al-Salem Station (latitude: 24°55'06", longitude: 55°10'32", elevation: 80 m, landuse: suburban, population density = 7 person km^{-2}) and D = Lahbab Station (latitude: 25°1'45", longitude: 55°36'48", elevation: 138 m, landuse: suburban, population density = 25 person km^{-2}).

4 Results and discussion

The performance of the GI for tropical and subtropical desert climates (Köppen Schemes, Bwh) over Dubai's high-density residential zones is provided in the summer and winter months, with a maximum air temperature of 40.2 °C and a minimum of 12.8 °C. The findings revealed that changing the surface vegetation could significantly impact

the city's energy balance. Assessments are made between the control run (the current urban climate) and scenarios (GI applied changed urban climate into all urban grid cells) across the city of Dubai to gauge the performance of city-scale modified GI. The specific findings are presented and evaluated.

4.1 Green infrastructure and heat flux

Extensive research, including significant numerical data, has been performed in recent years to analyze the implications of GI on urban energy balance. One of the most important components of city thermal environment management is the modification of urban energy balance. The reaction of GI varies based on the structure's urban building architecture, availability of the open spaces, and the city's layout. For all GI scenarios, the major surface energy partition, i.e., sensible and latent heat flow, is numerically analyzed and presented for different urban building environments i.e., low, medium, and high-density residential zones. The key components of energy balance, namely sensible heat, and latent heat, were evaluated and contrasted for each GI-based mitigation scenario. The fall in planetary boundary layer (PBL) height is typically influenced by reductions in surface sensible heat flow, and thermals from the urban surface as a result of substantial GI deployment over Dubai. For the summer month, the greatest sensible heat flux is determined to be peak solar time (14:00 LT), which is very near to 403.3 W m^{-2}, 489.5 W m^{-2}, 521.0 W m^{-2}, and 589.3 W m^{-2} for GI25, GI50, GI75, and GI100, respectively. For GI25, GI50, GI75, and GI100, the larger summer drop-in mean sensible heat as compared to the unmitigated scenario during peak hour (14:00 LT) is 39.2 W m^{-2}, 79.3 W m^{-2}, 102.3 W m^{-2}, and 149.3 W m^{-2}, respectively, over the average urban and high-intensity urban areas of the city. For GI25, GI50, GI75, and GI100, the mean reduction in sensible heat flux from the urban surface area are about 36.5 W m^{-2} (Jebel Ali, Jumeirah, Deira, and Bur Dubai), 82.6 W m^{-2} (some parts of Deira, Jebel Ali, and Bur Dubai), 91.2 W m^{-2}, and 123.3 W m^{-2} (Deira, and Bur Dubai), respectively, for the entire summer month. It represents a significant impending GI impact to reduce sensible heat and hold up the comfortable urban thermal environment on a city scale (Figure 4). At 14:00 LT, the maximum sensible heat flux is considerably lower and is about 312.7 W m^{-2}, 296.7 W m^{-2}, 278.2 W m^{-2}, and 257.8 W m^{-2}, whereas a comparable decline is found to be 62.6 W m^{-2}, 98.7 W m^{-2}, 113.2 W m^{-2}, and 135.6 W m^{-2} during the winter month. The loss of sensible heat from the urban surface in the winter months could consequence in a lower ambient temperature due to the harsh desert environment, but with the significantly higher temperatures in the city's dense regions throughout the winter month, the proportionate impact is substantial.

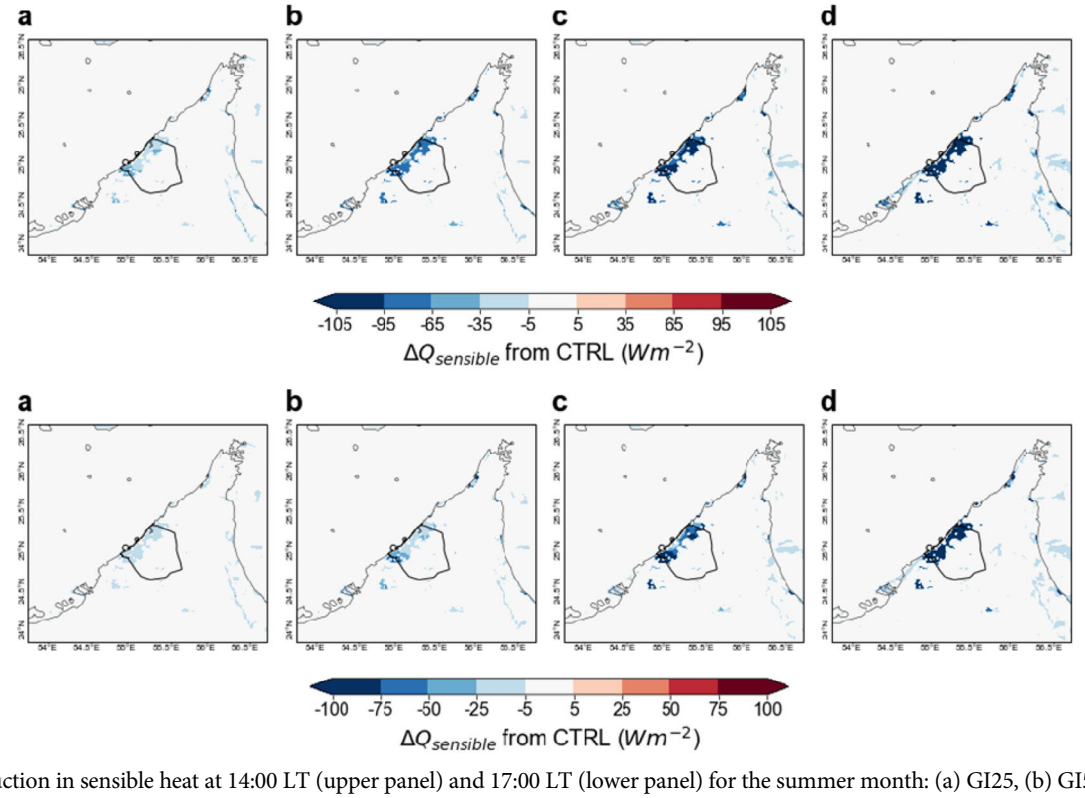

Fig. 4 Reduction in sensible heat at 14:00 LT (upper panel) and 17:00 LT (lower panel) for the summer month: (a) GI25, (b) GI50, (c) GI75, and (d) GI100

When evaluated in low and medium-density building environments, high-density residential areas showed a greater average drop in summer sensible heat flow. For example, the GI100 scenario's mean drop in summer sensible heat flux was 136.6 W m^{-2} for high-density regions and 98.2 W m^{-2} for low-density areas. This is due to increased vegetation-induced transpiration cooling and shadow effects in high and low-density residential areas, as well as soil moisture availability, which caused evaporation in low-density regions during peak sun hours. When vegetation patches are placed in an urban grid cell, the release of long-wave surface radiation to the outside environment is insufficient, resulting in the largest drop in surface temperature in high-density residential areas. On the other hand, the existing peri-desert ecology with xerophytes gathers around Dubai's medium-density residential zones. This surface features low-level evaporation and transpiration, as well as a variety of physiological systems for dealing with drought stress and producing in an unfavorable climate. This might also explain the small decrease in summertime sensible heat transfer in medium-density areas.

The highest summer latent heat at 14:00 LT is approximately 134.5 W m^{-2}, 203.4 W m^{-2}, 236.5 W m^{-2}, and 285.6 W m^{-2} for the four GI scenarios, while the higher increase of latent heat at 14:00 LT is 78.3 W m^{-2} (Jumeirah, Deira, and Bur Dubai), 153.2 W m^{-2} (some parts of Jumeirah, Deira, and Bur Dubai and northern parts of Dubai), 201.3 W m^{-2}. During the whole summer month, the average rise is between 76.3 W m^{-2}, 153.2 W m^{-2}, 203.2 W m^{-2}, and 232.6 W m^{-2} (Figure 5). During the winter season, minor fluctuations in latent heat are seen in Dubai. In terms of sensible heat, the proximity of Dubai creek during the summer provides a fondness for high-density urban zones to rise in latent heat over outskirt low-density zones. This is mostly owing to (a) urban and nearby open desert surface flux gradients, (b) moisture availability in the adjacent Arabian Gulf, and (c) high-intensity urban structures diverting ambient airflow, resulting in the city's buildings "lifting" warm, moist surface air into the colder lower atmosphere on top of it, where rain clouds can develop over the city's downwind or low-density urban parts (Khan et al. 2022b).

4.2 Green infrastructure and ambient temperature

The largest summer and winter decline in ambient temperature for various metropolitan zones were reported in Dubai at 14:00 LT. As a result, the peak sun hour (14:00 LT) was used as a proxy for temperature drop analysis since it corresponds to daytime throughout the simulation period reflecting the greatest ambient temperature decrease and potentially the biggest urban heating load in the urban

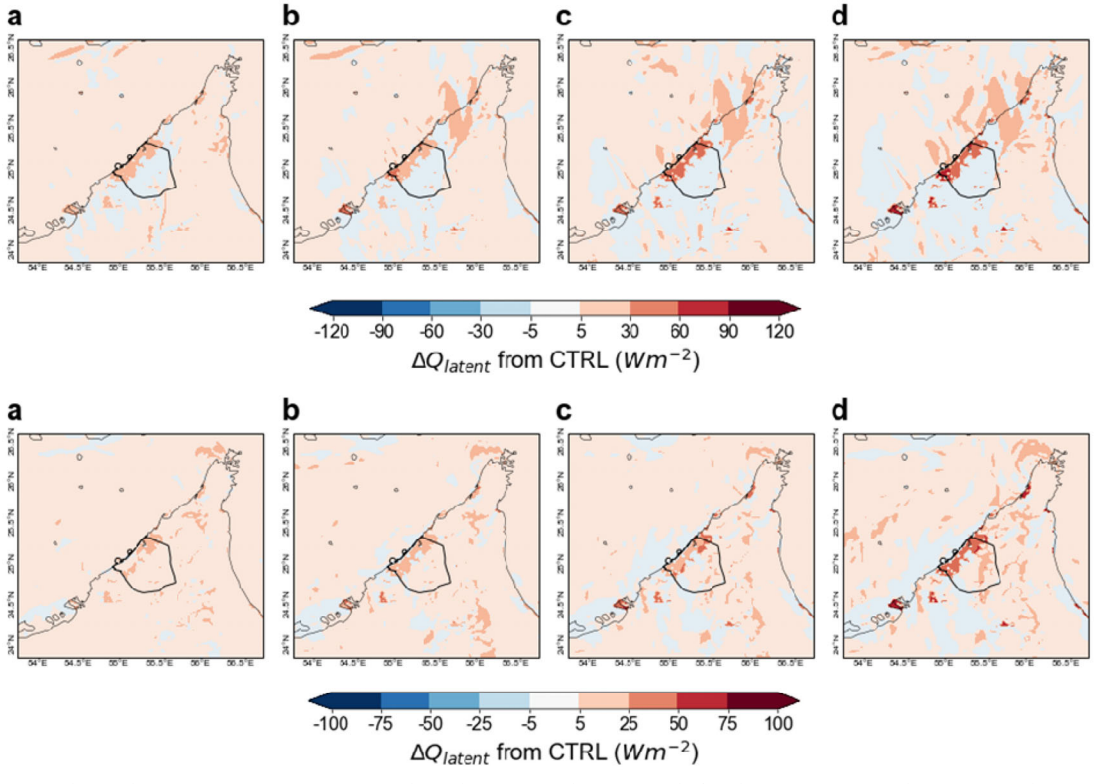

Fig. 5 Increase in latent heat at 14:00 LT (upper panel) and 17:00 LT (lower panel) for the summer month: (a) GI25, (b) GI50, (c) GI75, and (d) GI100

environment. Even if the GI hits 100% at peak hours, the maximum drop in average daily ambient temperature due to increasing urban vegetation patches in cities is limited to 1.7 °C (14:00 LT). During peak hours, the average fall in ambient temperature is close to 0.3 °C, resulting in a modest 25% increase in GI (14:00 LT). This type of proxy can reveal potential the expected temperature reduction induced by GI installation. The greatest decrease values were close to 0.6 °C, 1.1 °C, 1.4 °C, and 1.7 °C when GI25, GI50, GI75, and GI100 conditions were compared to the control condition, respectively. In all construction conditions, these values are more than the peak hour (14:00 LT) drop. The larger fall in summer ambient temperature at 15:00 LT for GI25, GI50, GI75, and GI100 scenarios is close to 0.5 °C, 0.9 °C, 1.3 °C, and 1.6 °C, respectively, when compared to the control condition. Throughout the summer month, the average ambient temperature drop for the four scenarios was 0.5 °C (Jumeirah, Deira), 0.7 °C (Jebel Ali and some areas of Jumeirah), 0.9 °C, and 1.2 °C (Jebel Ali, Jumeirah, Deira, and Bur Dubai) shown in Figure 6. During the winter, the highest reduction in ambient temperature at 15:00 LT is near 0.4 °C, 0.6 °C, 0.8 °C, and 1.1 °C, respectively, whereas the average drop in ambient temperature for the four GI scenarios is close to 0.2 °C, 0.4 °C, 0.6 °C, and 0.9 °C. Because dense building environments trap water vapor flux and urban trees shade at the lower level, high-density with leafy urban zones have a substantial drop in average temperature than medium and low-density zones. In high-density urban regions, for example, the average drop in ambient temperature for the high GI scenario, GI100, was 1.3 °C.

Daily temperature reductions are heavily influenced by the city's geography and surroundings. The temperature at night is significantly cooler than it is during the day. The expected temperature drops throughout the night, which are mostly achieved by the GI, are especially important since they help to cool down the city and lower the ambient temperature over the following several days. It also has a significant impact on human thermal comfort and surface energy levels at night. Even if the GI is increased to 100%, the largest attainable decline in average daily peak temperature attained by increasing urban vegetation cover in Dubai would be 1.2 °C. For a 25% and 50% increase in the GI, the average predicted peak temperature reduction is close to 0.6 °C and 0.8 °C, respectively. The largest ambient temperature fall associated with a 100% GI rise may not exceed 2.4 °C during the night; however, the temperature drop associated with a 25%, 50%, and 75% GI rise is close to 0.9 °C, 1.4 °C, and 1.9 °C, respectively. This is primarily because (a) an increased fraction of urban GIs perceptibly reduces the daytime accumulated heat in the urban environment while the subsequent release of stored heat from urban surfaces during the night, and (b) the rate of sensible heat released from vegetated surfaces during the

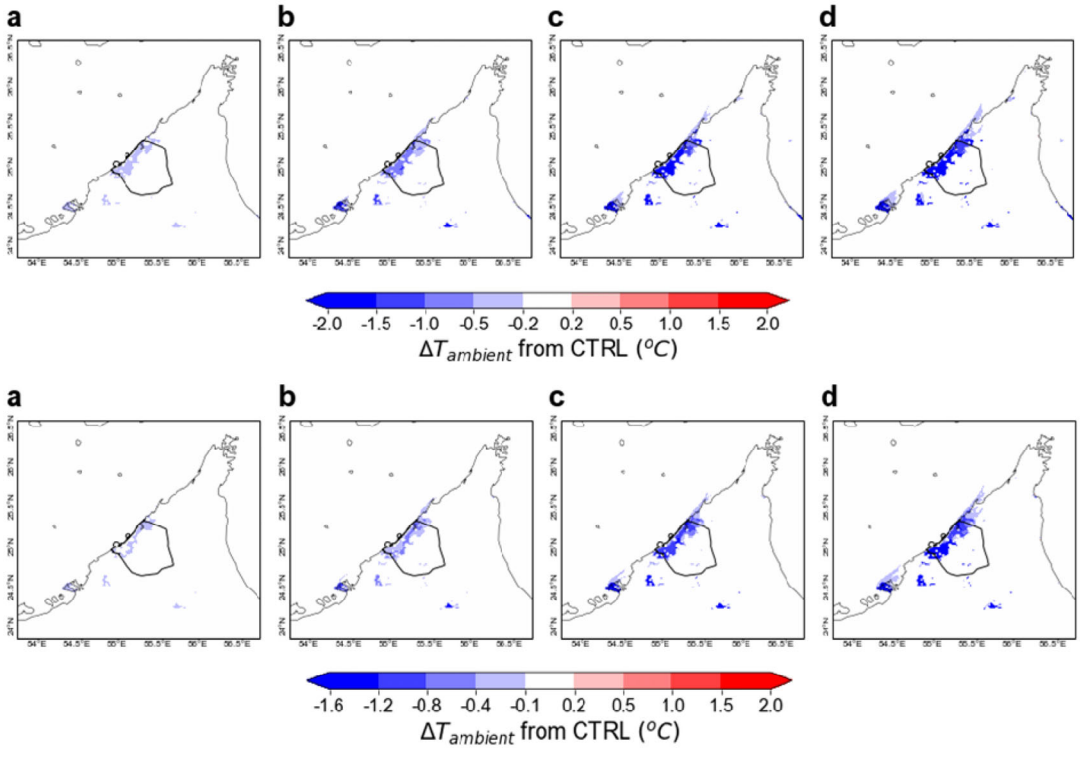

Fig. 6 Reduction in ambient temperature at 14:00 LT (upper panel) and 17:00 LT (lower panel) for the summer month: (a) GI25, (b) GI50, (c) GI75, and (d) GI100

night is significantly lower than the rate of corresponding heat released by impermeable urban surfaces during the day.

4.3 Green infrastructure and surface temperature

The greatest summer and winter drop in surface temperature was seen around 15:00 LT, coinciding with a reduction in ambient temperature. Summertime maximum decrease values for GI25, GI50, GI75, and GI100 scenarios were close to 1.9 °C (Jebel Ali, Jumeirah, Deira, Bur Dubai, and certain suburbs), 2.7 °C (Jumeirah and Deira), 2.9 °C, and 3.2 °C (Jebel Ali, Jumeirah, and Deira), respectively, compared to the control condition. The decline in surface temperature throughout the winter was up to 0.9 °C, 1.2 °C, 1.6 °C, and 2.2 °C at 17:00 LT for GI25, GI50, GI75, and GI100 scenarios, respectively. Furthermore, when comparing both seasons, these values are greater than the peak hour (14:00 LT) drop in all building settings. During the daylight peak hour (14:00 LT), transpiration is the major cooling process, and its influence on the surface energy balance is sufficient to compensate for and counterbalance sensible heat emission from impermeable surfaces in urban areas. The assigned humidity content of the urban surface in the model and the accessible humidity content of the lower atmosphere have a significant impact on the anticipated quantity of evaporative losses. Summer surface temperature reductions of 1.4 °C, 1.9 °C, 2.1 °C, and 2.7 °C were found at 14:00 LT for GI25, GI50, GI75, and GI100 scenarios, respectively, compared to the control condition. Summer average surface temperature reductions for the four scenarios are quite near-maximum dips of roughly 1.3 °C, 1.5 °C, 1.9 °C, and 2.4 °C, respectively (Figure 7). The maximum drop in surface temperature at 14:00 LT for the winter month for the selected GI-based urban cooling scenarios is close to 0.7 °C, 1.1 °C, 1.4 °C, and 1.6 °C, while the average decrease in surface temperature is close to 0.5 °C, 0.9 °C, 1.2, and 1.8 °C. Surface temperatures in Dubai's high-density residential districts fall considerably when compared to nearby medium and low-density residential regions.

4.4 Green infrastructure and relative humidity content

During the summer month's peak hour (14:00 LT), the relative humidity content is 59.2%, 62.1%, 70.2%, and 83.2% basis points for GI25, GI50, GI75, and GI100, respectively. When compared to the unmitigated scenario in the compact building zones of the urban area, the maximum summer augment of relative humidity at 14:00 LT under modified GI conditions is close to 2.8%, 3.5%, 8.6%, and 10.2% for the four scenarios, respectively (Figure 8), while the resultant increase of average humidity content is approximately 2.1% (Jebel Ali, Jumeirah, Deira, and Bur Dubai), 4.2% (Deira,

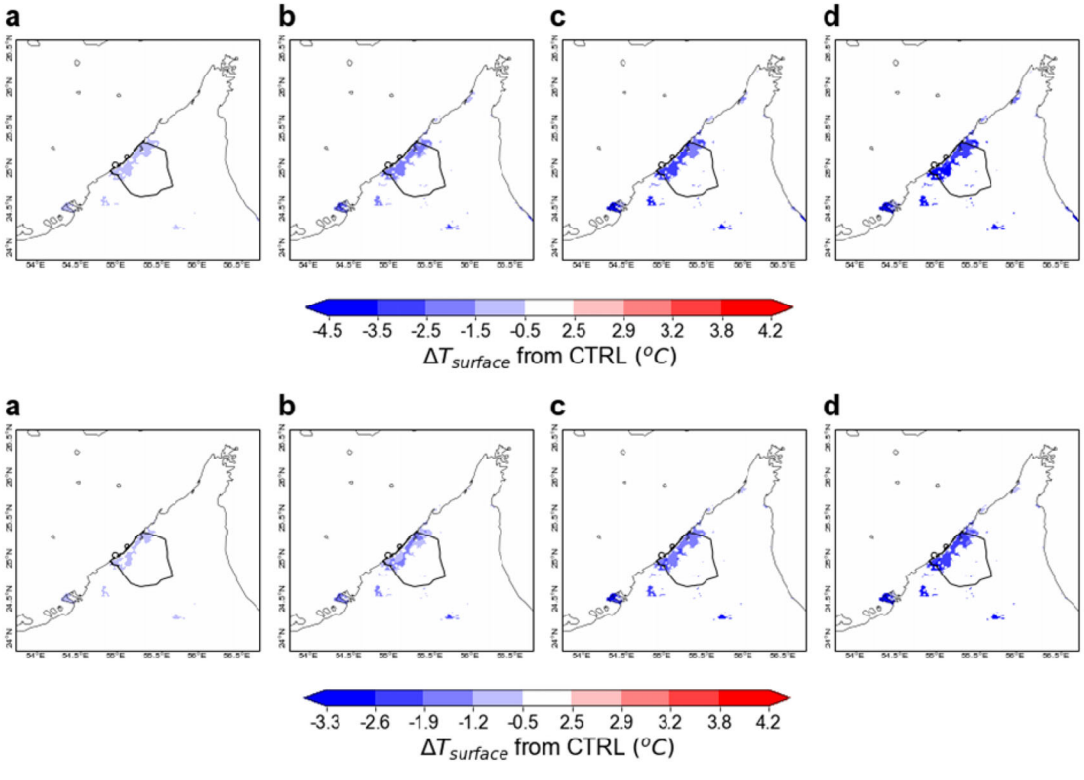

Fig. 7 Reduction in surface temperature at 14:00 LT (upper panel) and 17:00 LT (lower panel) for the summer month: (a) GI25, (b) GI50, (c) GI75, and (d) GI100

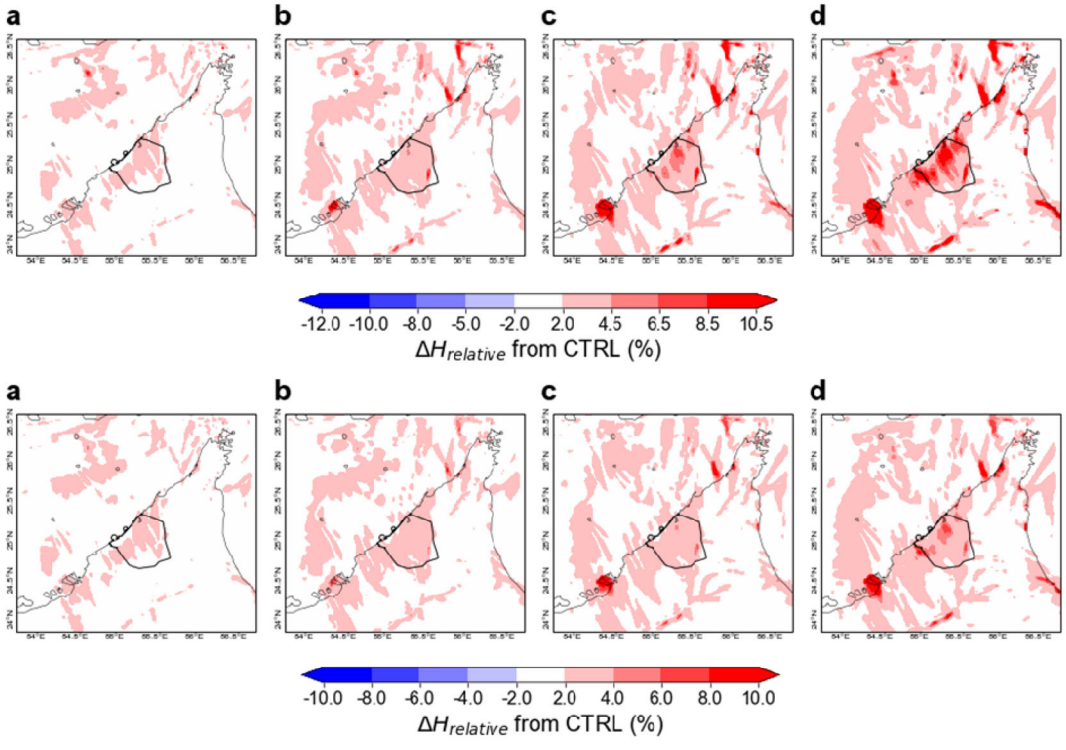

Fig. 8 Increase in relative humidity at 14:00 LT (upper panel) and 17:00 LT (lower panel) for the summer month: (a) GI25, (b) GI50, (c) GI75, and (d) GI100

and Bur Dubai), and 8.3% (Jebel Ali, Jumeirah, Deira, and Bur Dubai). The relative humidity content for the winter season is also quite consistent. Because of low-level water vapor flux dispersion into higher air, the city's high-density zones have high humidity content and a low sky-view factor due to leafy urban strictures. The usage of more urban plant patches in cities may raise ambient relative humidity, diminishing thermal comfort. Even in desert areas with low relative humidity content, a rise in ambient humidity levels generated by GI-based transpiration may provide a climatic advantage to urban dwellers.

4.5 Green infrastructure and wind speed

If the GI with trees is increased, the amplitude of wind speed changes shows a decreasing trend for the summer and winter months throughout the simulated days at the city scale (Figure 9). As a consequence of shade and transpiration cooling, increased GI cover may result in a decrease in temperature and surface wind speed in the lower PBL of the atmosphere. Because of the large fall in surface temperature, GIs may diminish wind speed, vertical mixing, and air dispersion in urban settings in the leafy urban structure of Dubai city. For the summer months, the average reduction in wind speed is roughly 0.5 m s^{-1}, 0.6 m s^{-1}, 0.9 m s^{-1}, and 1.3 m s^{-1} for GI25, GI50, GI75, and GI100, respectively, at 14:00 LT. The average drop in wind speed during the month of winter is smaller than during the summer months at 14:00 LT. A larger decrease in surface wind speed during summer months under the GI50 to GI 100 scenario is distributed to a greater extent across the entire urban area (Jebel Ali, Jumeirah, Deira, and Bur Dubai) due to higher GI, but not for the GI25 scenario, where the drop in wind speed was low and unequally distributed compared to preceding GI scenarios. During the winter month, the wind speed at 14:00LT was reduced by 0.4 m s^{-1}. This is because the magnitude of the wind speed has a substantial persuade on the surface temperature. Lower wind speeds show a downward trend in surface temperature due to the mechanical effects of turbulence. Given the larger decrease in surface temperature, the tendency is somewhat higher for a GI75 to GI100 rise in the GI. Furthermore, one of the most noticeable features of the desert environment is the rising diurnal temperature variations on a seasonal scale. The mounting turn down in night-time ambient temperature governs the outer urban environment.

4.6 Seasonal impacts of modified mesoscale urban green infrastructure

The GI is critical for improving cities' thermal environments. The increase of urban vegetation in the city through the mesoscale urban model altered the standard surface

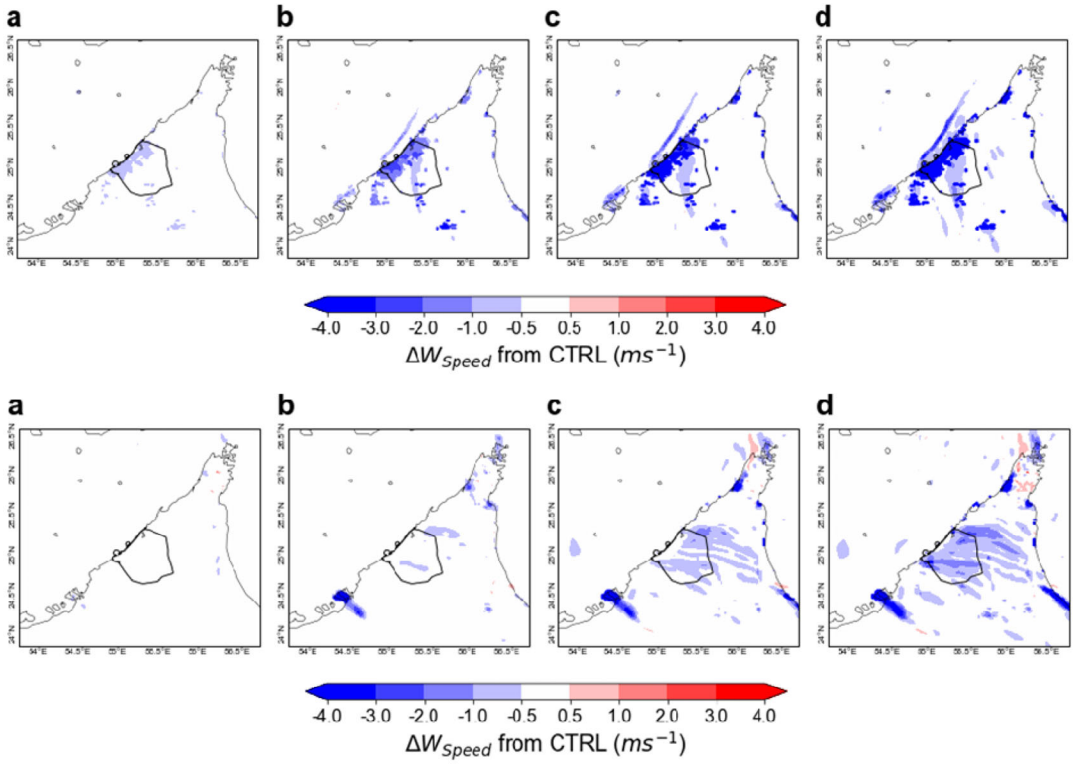

Fig. 9 Reduction in wind speed at 14:00 LT (upper panel) and 17:00 LT (lower panel) for the summer month: (a) GI25, (b) GI50, (c) GI75, and (d) GI100

meteorological fields, and urban energy budget in the lower urban atmosphere at a seasonal scale as well, this, in turn, has an impact on microclimate and surface radiation balance of the city. The changes in standard meteorological fields also persuade derived advective flows, and diurnal fluctuation in local convection in the urban area influences the transfer of warm or cold air from the immediately surrounding desert environment. In this section, analyses of mesoscale climatic impacts in the summer and winter months were presented. The results of 14:00 LT and 6:00 LT were also reported with temperature parameters and wind speeds for unmitigated and mitigated scenarios.

4.6.1 Green infrastructure impacts during the summer period at 14:00 LT

The magnitude of the projected peak daily ambient temperature reductions at 14:00 LT for four scenarios depicts in Figure 10. The average temperature reduction for scenarios of 25%, 50%, 75%, and 100% increase in green infrastructure is close to 0.39 °C, 0.59 °C, 0.82 °C, and 1.1 °C, respectively. Temperature declines of 0.5 °C, 0.6 °C, 1.1 °C, and 1.5 °C are the most significant, while temperature drops of 0.1 °C, 0.5 °C, 0.7 °C, and 0.9 °C are the least significant. For each 1% rise in the GI, the average temperature drops by 0.019 °C, 0.016 °C, 0.015 °C, and 0.011 °C, respectively. According to a study of forty-six similar investigations given in Santamouris and Osmond (2020), the corresponding average decline was close to 0.017 °C, which is pretty similar to the current results.

In the reference case, wind speed has a negligible influence on peak ambient temperature during peak hours. The drop in wind speed is determined by the significant fall in surface temperature. This is because desert winds in Dubai are greatly hampered by regional highs above the city due to enhanced transpiration cooling and shadow effects. Stagnant conditions and warm surface advection are associated with low wind velocity. For the four higher GI situations, the relationship between wind speed and peak ambient temperature is comparable. This relationship between ambient temperature and wind speed during peak hours (14:00 LT) is shown to have a significant impact on the additional GI's mitigating efficacy. In reality, the more vegetation there is, the smaller the temperature drops caused by it. As indicated, for every degree of temperature rise, the peak temperature decrease under GI circumstances is lowered by 0.017 °C. This is significant because it relates to the variation in sensible and latent heat released as a function of surface wind and advective flow. This becomes clear when the association between prolonged wind speed and temperature decline is shown, as well as the relationship between the Bowen ratio and wind speed (Figure 11). As previously stated, the little fluctuation in temperature decrease

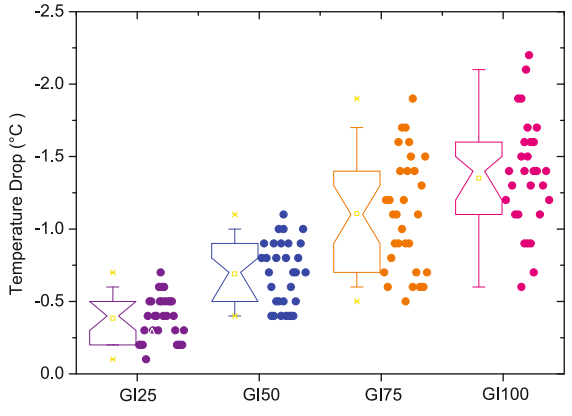

Fig. 10 Box plots of the maximum temperature drop at 14:00 LT for three scenarios of GI increases for whole urban domain (d03)

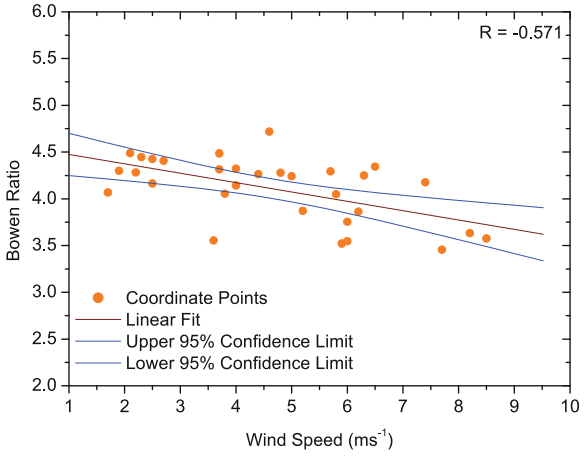

Fig. 11 Association between wind speed and corresponding Bowen ratio is used to describe the type of heat transfer for a surface that has moisture available at 14:00 LT for GI100 scenario

as a function of ambient temperature and wind speed illustrates the variability of the Bowen ratio versus wind speed.

During 14:00 LT, a rise in the GI was noticed to have reduced the average wind speed in the city. This is because of the increased roughness length caused by replacing urban grids with GI, which, when paired with existing buildings and trees, may divert wind downhill, despite a drop in surface heating, which leads to a fall in surface temperature. When the GI increases by 25%, 50%, 75%, or 100%, the mean wind speed at 14:00 LT decreases by 12%, 17%, 24%, and 32%, respectively, compared to the reference scenario.

During the summer peak daily time, the expected increase in the city's GI lowers the surface temperature. While the average surface temperature is similar to 38 °C under reference circumstances, it decreases by 0.9 °C, 1.2 °C, 1.5 °C, and 2.6 °C for the four additional GI situations, respectively. The reference surface temperature has a significant linear association with the results for the four scenarios, as predicted. The average percentage drop ranged between 2% and 7%. Each scenario demonstrates a significant linear connection between ambient and surface temperature, with regression slopes that are quite comparable. The increasing GI fraction has a significant impact on surface temperature. With a higher proportion of GI, the surface temperature has a considerably lowering tendency. Given the lower surface temperatures, the tendency is substantially greater under a 100% rise in the GI. At low wind speeds, the average surface temperature in the four scenarios is usually comparable.

It has been revealed that the fraction of modified GI improves sensible heat loss. While the average sensible heat flow was equivalent to 341.4 W m^{-2} for reference values, it rose to 373.5 W m^{-2}, 412.5 W m^{-2}, 438.3 W m^{-2}, and 485.7 W m^{-2} for the 25%, 50%, 75%, and 100% GI situations, respectively. This is owing to a large fall in surface temperature as GI rises, despite a decrease in wind speed. The average magnitude of latent heat under reference conditions was close to 65.7 W m^{-2}, increasing to 135.5 W m^{-2}, 198.7 W m^{-2}, 212.3 W m^{-2}, and 261.7 W m^{-2} for the four GI scenarios of 25%, 50%, 75%, and 100%, respectively. The level of latent heat at 14:00 LT varied considerably for each scenario during the study, and its relationship with ambient temperature and wind speed was shown to be rather significant. While the Bowen ratio was close to 0.21 under reference settings, it climbed to 0.39, 0.47, 0.56, and 0.77 under the 25%, 50%, 75%, and 100% conditions, resulting in a significant reduction in ambient temperature. The average relative humidity increased from 37.8% under reference conditions to 43.2%, 49.5%, 53.6%, and 61.2% for the 25%, 50%, 75%, and 100% scenarios, respectively, due to the considerable increase in latent heat flux.

4.6.2 Green infrastructure impacts during the summer period at 6:00 LT

The unmitigated scenario and the early morning hour show a very weak association between ambient temperature and wind speed. Wind speeds at 6:00 LT are typically modest, seldom topping 1.2 m s^{-1}, apart from one day. The lower the wind speed, the greater the fall in ambient temperature since the fetch wind from the Arabian Gulf is cooler. The average temperature reduction caused by an increase in the GI was close to 0.2 °C, 0.5 °C, 0.7 °C, and 1.1 °C for the 25%, 50%, 75%, and 100% GI scenarios, respectively. While the temperature reductions during the peak daily ambient temperatures were comparable in the first, second, and third scenarios. Temperature decreases for GI100 were much greater in the early morning than throughout the peak day. Previous research has found that the projected temperature decline driven mostly by urban GI is greater at night. When the reference ambient temperature is raised, the average

temperature drops considerably. Because greater ambient temperatures correlate to lower wind speeds and less advective cold air out of the city's desert fetch, additional transpiration cooling contributes less to the overall thermal balance.

4.6.3 Green infrastructure impacts during the winter period at 14:00 LT

Increased urban GI has been demonstrated to significantly reduce the city's peak ambient temperature during summer. The reduction in mean ambient temperature for the four GI scenarios at 14:00 LT was close to 0.2 °C, 0.4 °C, 0.6 °C, and 0.9 °C, respectively. Reduced wind speeds lead to a significant drop in temperature. Lower wind speeds in the urban domain enhance the sea breeze of cooler air from the Arabian Gulf, resulting in a considerable reduction in evapotranspiration's thermal influence on the thermal balance. For the same reason, lower wind speeds are claimed to correlate to lower ambient temperatures under the reference conditions. In reality, a reduction in wind speed translates to a lower surface temperature as well as a larger temperature drop due to the city's enhanced GI.

4.7 Impacts of enhanced green infrastructure on the lower atmosphere

The increased GIs can change both the radiative and non-radiative components of leafy building urban environments. The effect of leafy buildings on horizontal scales, building energy balance, roughness elements, horizontal advection of heat and momentum, and inertial sub-layer or boundary layer blending height (whichever is greater) is directly connected to modified GI. The rise in the GI from 50% to 100% is due to competing for biophysical processes on the city's surface energy budget and available moisture contents, which alters the lower atmospheric boundary layer dynamics during peak hours (14:00 LT). The urban-scale GIs may also have exaggerated features like reflectivity properties of the surface, vertical wind profiles, and leaf area index (LAI), which drive urban heat and moisture fluxes throughout the whole city of Dubai under scenarios of 25%, 50%, 75%, and 100% GIs. Heat flux differences can have an impact on pressures, dynamics, and PBL lowering over Dubai's GI-implemented city. It has been observed that increasing GIs from 50% to 100% can increase the leave go of lower atmospheric water vapor fluxes into the air by 6%–12% during the day. Consequently, the surplus urban heat advection diminishes, resulting in increased latent heat flux and lower atmospheric available moisture content (up to 12%) in the lower atmosphere of the urban domain of Dubai city during the day when incoming solar energy is at its maximum. Increased boundary layer humidity may promote cloud formation in the lower atmosphere and convectional rain in the afternoon. Higher GIs subordinate the altitude of the boundary layer of the urban atmosphere (up to 486 m above the major metropolitan region) in comparison to the control case simulation, the lowest portion of the atmosphere that is most susceptible to the collective stroke of mechanical and thermal stimuli (Figure 12). Clouds are predicted to change the quantity of incoming solar radiation that reaches the lower atmosphere, influencing the surface energy balance of the city and perhaps causing precipitation in a few locations of Dubai (downwind). It is demonstrated that feedback between the lower atmospheres and rising GIs (i.e., 25%, 50%, 75%, and 100%) may be significant; amplification may rise from 16 to 43% of the inconsistency in urban surface energy as well.

Furthermore, the results demonstrated that the changeability in GIs fractions, i.e., a low GI fraction to maximum GI limit (i.e., 25%, 50%, 75%, and 100%), and thus surface heat fluxes, could escort to spiky ascents in temperature dynamics in the PBL surface, which might force to augment the limited inland circulations like "sea breezes" over the urban atmosphere. As a result, during mesoscale urban greening, the separation of urban heat fluxes i.e., sensible and latent heat (i.e. Bowen ratio) is directly associated with the number of vegetation fractions. This was most noticeable in the GI100 when compared to GI25, GI50, and GI75 scenarios. The impacts of mesoscale urban greening at the urban scale significantly alter the onset of the sea breeze from the Arabian Gulf and augment thermally induced upslope flow during peak solar hour (14:00 LT), and the likelihood of the appearance of assorted urban scale circulations owing to the different fraction of GIs was also presented from urban domain to immediate coastal area (Figure 12). The flow of sea breeze from the Arabian Gulf, according to the findings, is candidly associated with the intensity, amplitude, and spatial pattern of urban heating grades in the city of Dubai, because additional vegetation in the location of the city pocket implies not as much of urban heat at the peak solar time. As a result, the distinctiveness of sea breeze circulation from the Arabian Gulf is possible to be held back due to the existence of GIs. The privileged urban areas with GI fraction near the proximity of the water bodies (Dubai Creek or inland water) create an added pitch of latent heating through transpiration cooling, reducing sea breeze penetration into Dubai's metropolitan core. As a result, the outflow of the sea breeze boosts the specific humidity (up to 12.7 g/kg) across the metropolitan zone. Aerodynamically, GIs produce an uneven surface that slows both surface and vertical wind (up to 1.8 m s^{-1}) by rooting turbulence on top of the tree canopy. It should be noted that Dubai had the mechanical forcing towards sea

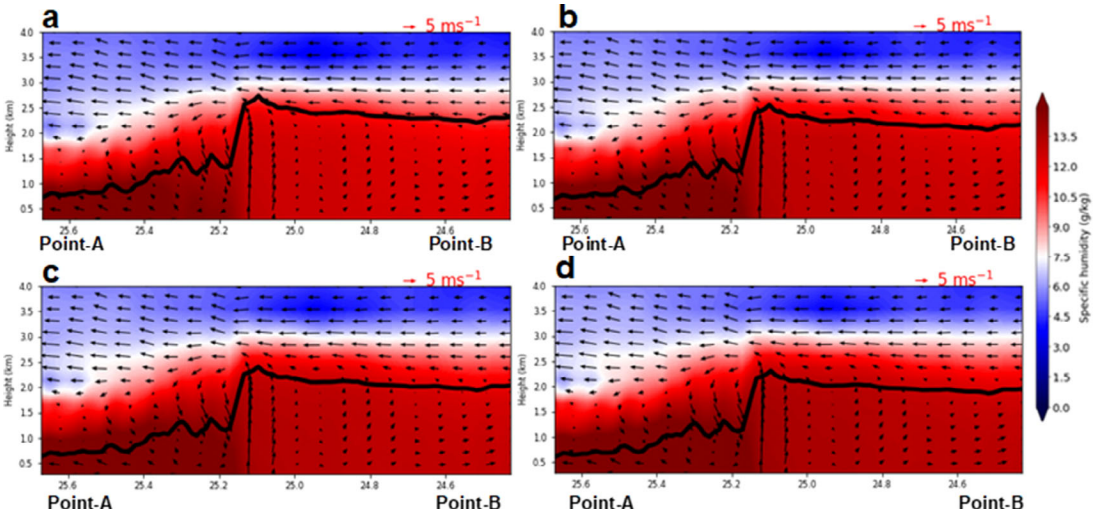

Fig. 12 Cross-sectional profile of GI at 14:00 LT for the summer month: (a) GI25, (b) GI50, (c) GI75, and (d) GI100. Thick black lines show PBL height distribution and corresponding changes in vertical wind speed and specific humidity. Increased vegetation cover from GI25 to GI100 considerable alters the vertical wind profile. The sensitivity experiments suggest that the PBL is sensitive to the availability of moisture through transpiration cooling in the lower atmosphere. While the additional vegetations cover is a sensitive indicator at the surface, it also has an impact on the surface energy and hydrologic balance over the urban domain

breeze circulations during peak solar time due to transpiration cooling of the GIs. Furthermore, in metropolitan areas, the 50-100% GIs scenario noticeably dwindles the ambient temperature during the nocturnal hours compared to daytime, which may have impacted the land breeze. Because added mesoscale urban greening in Dubai city may generate higher UHI at night. In addition, the vegetation has higher inertia in the urban environment during the day, while the nighttime land breeze may be altered and prolonged.

The large-scale synoptic meteorological background, which is crucial in regulating the prevailing wind at the urban surface, largely determines the strength of sea breeze circulation. The findings revealed that the height of the PBL in Dubai is directly connected to the vertical advection of the sea breeze. When GI is used in city size, the circulation pattern may change. The GI might alter the PBL height, resulting in confined circulation over Dubai's urban area. The effect of the "regional high" inside the lower PBL, as well as the offshore synoptic wind flow above the PBL, delayed the introduction of the sea breeze throughout the afternoon (14:00 LT). The denser cold air above the urban domain flows towards the suburban zone to replenish the buoyant warm air. GI approaches can limit vertical lifting of urban thermals, conveyance and dispersion of low-level motions, and delay the sea wind front in hot summer. As a result, vertical wind speed coverage decreases by 1.3 to 3.2 m s^{-1}, signifying more subsidence over the metropolitan zone. The surface roughness features are painstakingly calibrated to benefit from mixing effects in bringing cold air from sea breezes down to the surface. Furthermore, the increased degree of surface roughness components may create horizontal wind shear and frontal lifting; delaying the beginning of the sea breeze front into the city's core urban zone. The effectiveness of sea breeze advection is largely affected by the size and shape of the city, which determines the impact of urban heating. Thus, GI for Dubai city areas has had a significant impact on the thermal and kinetic profiles of the PBL and sea breeze circulation. This synoptic surge occurs in the opposite direction of the sea wind, making the created sea breeze front more sensitive to the buildup of harmful secondary pollutants at the back of the front.

The application of GI at the city scale can significantly alter the pressure differential between the city and the surrounding surface due to a large reduction in the ambient temperature of up to 1.7 °C and a decrease in wind speed of up to 1.3 m s^{-1}. Thus, variations in GI, sensible heating, and wind cause feedback within the city's local climate during peak hours (14:00 LT). Higher urban GI values reduce advective flow between the city and its environs, increasing cooling potential. It produces a "regional high", which affects both horizontal and vertical wind speed across the city. The airflow pattern in a green urban area is typically determined entirely by the approximate length of the buildings. Vegetation not only reduces horizontal wind components but also increases downward wind velocity. Airflow may be directed downward by urban vegetation, just as it can be directed upward by shrubs or tiny plants. As a result, the region around buildings may experience significant wind velocity and turbulence, which can cause discomfort at ground level. At 14:00 LT, the average drop in wind speed in the desert and seaside is 0.9 and 1.2 m s^{-1},

respectively. As a result of the influence of this regional high over the urban domain, the rise in GI may prevent warm airflow from the nearby desert from reaching the downtown area (Figure 12). Furthermore, it is demonstrated that the influence of the sea wind is significantly diminished over high-density residential areas.

5 Comparison with previous studies: continental scale to city-scale

A city-scale increase in the GI can provide adequate thermal compensation for unwarranted urban pollution, city temperature, the economy, and health. Santamouris and Osmond (2020) thoroughly evaluated fifty-five large-scale GI-based scenarios and city-specific case studies to examine the overall impact of rising cities' GI on ambient temperature, urban pollution, and health for thirty-nine cities located across continents and climatic zones. Rising GI possesses a substantial effect over the peak diurnal temperature outline of cities, according to their results, and temperature drops during the night and day may not surpass 2.3 °C and 1.8 °C, respectively, even if the GI increases by 100% in the cities. These results, however, are entirely reliant on model parameterization methods, the amount of green area, city architecture, geography, temperature, building typology, and other variables.

For comparison purposes, forty-six large-scale GI-based research were included to understand the effect of increasing vegetation cover in thirty urban areas (Khan et al. 2022b). The locations and localities of each research were reviewed and statistically reported in a thorough manner (Santamouris and Osmond 2020). The study almost entirely covered North America (Detroit, Dallas, New Orleans, New York, Toronto, Philadelphia, and North-eastern parts of the United States), South America (Sao Paulo), Oceania (Brisbane, Darwin, Melbourne, Parramatta, and Sydney), Europe (Bochum, Stuttgart, and Vienna), and Asia (Hong Kong, Singapore, and Tehran). The data from these cities were carefully evaluated and numerically compared with the current study for scientific acceptability.

The GI ratio ranged from 1.3% in New York's Bronx to 100% in Melbourne and Hong Kong, according to the findings of the proposed large-scale GI-based heat reduction initiative. It has also been calculated that the average rise of GIs in cities was close to 22%; however, this is dependent on actual or hypothetical circumstances. In this study, a close to 25% of the known GI assumptions was utilized to derive Eqs. (1) and (2). The observed nonlinearity between temperature decrease and urban GI cover is consistent with the experimental results, where it was observed that the temperature decrease caused by greenery was a nonlinear function of increasing canopy cover, with higher cooling when the GI cover exceeded 25%. Based on known GI assumptions, we utilize a simple statistical correlation between maximum daily ambient temperatures at 15:00 LT and the average temperature decrease throughout the night with an increased proportion of GIs in the city to different continental scales.

The maximum daily temperature decline at 15:00 LT ($\Delta T_{15:00\text{LT}}$) can be estimated by using Eq. (1)

$$\Delta T_{15:00\text{LT}} = d\Delta\text{GI} \tag{1}$$

where ΔGI is shown as %, d = 0.0174, and the coefficient of determination (R^2) is very close to 0.90.

Also, the average night-time temperature drop, ΔT_{night} can be calculated by using Eq. (2)

$$\Delta T_{\text{night}} = d_1\Delta\text{GI} \tag{2}$$

where d_1 = 0.0331 and the coefficient of determination (R^2) is very close to 0.76.

In Figure 13, Lines 1 and 3 give the projected peak daily temperature and average night-time temperature relation, respectively.

Parameters ΔT_{night} and $\Delta T_{15:00\text{LT}}$ were estimated for all GI scenarios of the current study, Lines, 2 and 4 of the following Figure 13 show the estimated mean variability of the two parameters in the urban area of Dubai. In Dubai, the slope d of the daytime peak decline is nearly equal to 0.0168, compared to 0.0174 in Eq. (1). In comparison, the average slope of d_1 at night in Dubai is near 0.0432, as compared to 0.0331 in Eq. (2). The peak daytime and nighttime changes of the ambient temperature in Dubai are quite near to the average values observed in the forty-six

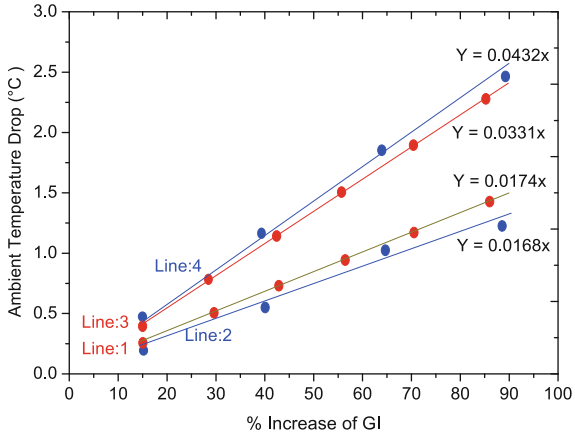

Fig. 13 Plot of the peak day time and average night time ambient temperature as a function of increase of the local GI. Line 1: as proposed by Eq. (1) for the peak day time ambient temperature. Line 2: calculated average drop of the peak daytime ambient temperature in Dubai. Line 3: as proposed by Eq. (2) for the night-time ambient temperature, and Line 4: calculated average drop of the night ambient temperature in Dubai

previous studies and the range suggested by the previous studies.

Desert cities are commonly subjected to the effects of regional climate change. Cities may acclimate by improving their urban GI to lessen the effects of severe urban heat through transpiration cooling. In this scenario, mesoscale urban GI simulations using the WRF-SLUCM are influenced by the physical parameterization in the model. The mesoscale climate model includes several parameterization methods that may readily mimic the coupled feedback process between the lower atmosphere and the land surface. A numerical analysis was undertaken with several parameterization approaches for the city of Stuttgart, and important discrepancies in numerical findings were found when compared to other cities (Fallmann et al. 2013).

The extent of the change in urban energy balance and the resulting decrease in ambient temperature is fully dependent on specific geographical location, climate, urban shape, parameterization approaches, and the quantity of new urban GIs deployed. With different vegetated patches (mosaic) of different urban vegetation implemented completely on a certain portion of each urban grid cell in the model domain, higher transpiration or evapotranspiration resulted in excellent cooling and less excess heat during peak solar hour, and thus a noticeably lower nocturnal ambient temperature in Dubai (Zoulia et al. 2009). Similarly, when GIs are encircled by impermeable surfaces, the pocket of high anthropogenic heat sources, or extremely close to desert fetch, cooling performance suffers because of excessive warm advection (Helling and Rienow 2021). However, before applying any heat mitigation measures, the sensitivity searches for ambiguity about the model assumptions and precision while coupling and assessing the unambiguous geographic circumstances of the cities must be evaluated.

6 Conclusions

The numerical efficiency of the mosaic-based urban vegetation patches as GI strategies for mitigating the effects of high urban temperatures in Dubai is explored and reported. When compared to the control scenario, the daily peak fall at 17:00 LT for ambient temperature is nearly equal to 0.0168 °C, while the maximum predicted summertime daily temperature decline for GI25, GI50, GI75, and GI100 scenarios, respectively, is very close to 0.6 °C, 1.1 °C, 1.4 °C, and 1.7 °C. For the GI100 scenario, the proportional drop in night-time ambient temperature per unit rise in the GI is determined to be 0.0432 °C; with a maximum temperature, the reduction is around 2.4 °C. Implementing GI in cities, according to new research, can noticeably reduce peak day and overnight ambient temperatures while also enhancing the quality of the global environment. The degree of cooling given by greater urban GI, on the other hand, varies greatly depending on topography, the presence of heating or sinking zones of urban heat in the surrounding environment, the kind of vegetation, synoptic conditions, and other meteorological and urban variables. According to studies, urban greenery lowers ambient temperature substantially more at nighttime as compared to daytime, with an average lowering rate of close to 0.0168 °C and 0.0432 °C per unit increase in GI infrastructure during the daytime and, nighttimes, respectively. The data also show that the temperature decrease in Dubai is quite comparable to the average from the compared research, despite a few days showing a greater decrease due to the impact of the sea breeze and diurnal weather variation due to its proximity to the Arabian Gulf and long fetch desert environment.

An increasing degree of GI has been shown to have a substantial effect on the thermal balance of the city. Lower surface and ambient temperatures encourage secondary advective flows, and diurnal fluctuation in local convection in the urban area influences the transfer of warm or cold air from the immediately surrounding desert environment. Lower surface temperatures and global airflow disturbances have been observed to dramatically reduce the height of the PBL (up to 468 m above the main metropolitan zone), potentially increasing ground-level air pollution. Lower PBL heights as a result of GI-based urban cooling, as well as an increase in biogenic volatile organic compound (BVOC) emission from increased vegetation, might have a significant impact on air pollution levels. Due to increased transpiration cooling and shadow effects, as well as a likely delay of the sea breeze, there is a rise in humidity in Dubai. As a result, their impact on thermal comfort may be studied in the future.

The study does not account for considerable neighborhood-level urban green infrastructures. This point could be a weakness in the present study. It is outside the scope of our investigation because we looked at the performance of various GI conditions on a city scale. We recommend future investigation at the neighborhood scale using WRF in conjunction with any microscale offline model. Another concern is that additional research is needed to understand the shift in GI cooling potential during heat waves and high temperatures. It has been proved that GI can offer less urban cooling or even drop the ambient temperature below a particular threshold or critical temperature. Considering the continued growth in the amplitude and frequency of high urban heat, the precise microclimatic effect of GI, and the mitigation powers of an added GI during extreme urban heating conditions remain unsolved questions that need to be investigated further. Furthermore, a comprehensive approach is advised for future study, i.e., the detailed classification of the urban

terrain in a practical way, as well as the examination of the complete cost and advantages of GIs in urban areas.

Furthermore, there is significant uncertainty in existing mesoscale urban climate models regarding simulation assumptions, parameterization schemes, and correctness in the sequence of coupling and evaluation of particular surface conditions, building morphology, and urban heating characteristics in cities. A numerical model's predictive capacity can be improved by calibrating the sensitive or ensemble parameters that have a substantial effect on model predictions. Even if the physics that underpins these models is universal, the absence of appropriate data or model assumptions that reflects the urban environment in climate-relevant terms for climatic models is a significant impediment to progress. Furthermore, a long-term climate-based urban categorization system protocol is also required to classify cities' urban environments into neighborhood types that can guide parameter selection in model applications. Future study would aim to improve surface meteorological conditions predictions by calibrating WRF model parameters for urban heat mitigation simulations with improved surface conditions and model physics. The calibrated parameters' endurance may be tested over a variety of boundary conditions and grid resolutions. Because of a set of physics choices and model dynamics within the WRF model, dynamic downscaling of general circulation model (GCM) data for any region is now feasible. Advances are also required to increase the capture of actual urban energy balance in cities, get higher spatial and temporal resolutions, and improve accuracy at the neighborhood scale. These will have a substantial impact on the forecast of urban green infrastructure based cooling capacity. This enables us to better develop adaptation and mitigation plans, hence reducing negative warming repercussions.

Acknowledgements

The authors are indebted to the mesoscale climate modeling community for their remarkable scientific efforts to develop the WRF model. The authors are also dully acknowledged to the European Centre for Medium-Range Weather Forecast (ECMWF 2011): ERA-Interim reanalysis dataset, Copernicus Climate Change Service (C3S) for providing meteorological inputs for forcing the WRF model.

Funding note: Open Access funding enabled and organized by CAUL and its Member Institutions.

Declaration of competing interest

The authors have no competing interests to declare that are relevant to the content of this article.

Author contribution statement

All authors contributed to the study conception and design. Material preparation, data collection and analysis were performed by Afifa Mohammed, and Ansar Khan. Supervision, project administration, and conceptualization were executed by Mattheos Santamouris. The first draft of the manuscript was written by Afifa Mohammed, and Ansar Khan and all authors commented on previous versions of the manuscript. All authors read and approved the final manuscript.

References

Abaas ZR (2020). Impact of development on Baghdad's urban microclimate and human thermal comfort. *Alexandria Engineering Journal*, 59: 275–290.

Aboelata A, Sodoudi S (2020). Evaluating the effect of trees on UHI mitigation and reduction of energy usage in different built up areas in Cairo. *Building and Environment*, 168: 106490.

Abu Ali M, Alawadi K, Khanal A (2021). The role of green infrastructure in enhancing microclimate conditions: a case study of a low-rise neighborhood in Abu Dhabi. *Sustainability*, 13: 4260.

Abu Dhabi Department of Planning and Municipalities (2010). Abu Dhabi Public Realm Design Manual.

Akbari H, Pomerantz M, Taha H (2001). Cool surfaces and shade trees to reduce energy use and improve air quality in urban areas. *Solar Energy*, 70: 295–310.

Akbari H, Cartalis C, Kolokotsa D, et al. (2015). Local climate change and urban heat island mitigation techniques – the state of the art. *Journal of Civil Engineering and Management*, 22: 1–16.

Al-Sallal KA, Al-Rais L (2012). Outdoor airflow analysis and potential for passive cooling in the modern urban context of Dubai. *Renewable Energy*, 38: 40–49.

Andersson E, Langemeyer J, Borgström S, et al. (2019). Enabling green and blue infrastructure to improve contributions to human well-being and equity in urban systems. *BioScience*, 69: 566–574.

Aram F, Higueras García E, Solgi E, et al. (2019). Urban green space cooling effect in cities. *Heliyon*, 5(4): e01339.

Benedict MA, McMahon ET (2002). Green infrastructure: smart conservation for the 21st century. *Renewable resources journal*, 20(3): 12–17.

Bolleter J (2014). Reconnecting Dubai with its landscape. *Landscape Architecture Australia*, 141: 14–20.

Chatzinikolaou E, Chalkias C, Dimopoulou E (2018). Urban microclimate improvement using envi-met climate model. *The International Archives of the Photogrammetry, Remote Sensing and Spatial Information Sciences*, XLII-4: 69–76.

Chen F, Dudhia J (2001). Coupling an advanced land surface–hydrology model with the Penn state–NCAR MM5 modeling system. Part I: Model implementation and sensitivity. *Monthly Weather Review*, 129: 569–585.

Chen F, Kusaka H, Bornstein R, et al. (2011). The integrated WRF/urban modelling system: development, evaluation, and applications to urban environmental problems. *International Journal of Climatology*, 31: 273–288.

Connop S, Vandergert P, Eisenberg B, et al. (2016). Renaturing cities using a regionally-focused biodiversity-led multifunctional benefits approach to urban green infrastructure. *Environmental Science & Policy*, 62: 99–111.

Conway TM, Khan A, Esak N (2020). An analysis of green infrastructure in municipal policy: Divergent meaning and terminology in the Greater Toronto Area. *Land Use Policy*, 99: 104864.

Coutts AM, White EC, Tapper NJ, et al. (2016). Temperature and human thermal comfort effects of street trees across three contrasting street canyon environments. *Theoretical and Applied Climatology*, 124: 55–68.

Cowan T, Purich A, Perkins S, et al. (2014). More frequent, longer, and hotter heat waves for Australia in the twenty-first century. *Journal of Climate*, 27: 5851–5871.

European Environmental Agency (2011). Green Infrastructure and Territorial Cohesion. European Environmental Agency (EEA), Copenhagen, Denmark.

Fallmann J, Emeis S, Suppan P (2013). Mitigation of urban heat stress—A modelling case study for the area of Stuttgart. DIE ERDE–Journal of the Geographical Society of Berlin, 144(3–4): 202–216.

Foster J, Lowe A, Winkelman S (2011). The Value of Green Infrastructure for Urban Climate Adaptation. Washington, DC: Center for Clean Air Policy.

Founda D, Santamouris M (2017). Synergies between urban heat island and heat waves in Athens (Greece), during an extremely hot summer (2012). *Scientific Reports*, 7: 10973.

Fu J, Dupre K, Tavares S, et al. (2022). Optimized greenery configuration to mitigate urban heat: A decade systematic review. *Frontiers of Architectural Research*, 11: 466–491.

Guinn TA, Mosher FR (2015). Numerical model derived altimeter correction maps for non-standard atmospheric temperature and pressure. *International Journal of Aviation, Aeronautics, and Aerospace*, 2(2): 4.

Gao K, Santamouris M, Feng J (2020). On the cooling potential of irrigation to mitigate urban heat island. *Science of the Total Environment*, 740: 139754.

Givoni B (1989). Urban Design in Different Climates. WMO: World Meteorological Organization.

Gunawardena KR, Wells MJ, Kershaw T (2017). Utilising green and bluespace to mitigate urban heat island intensity. *Science of the Total Environment*, 584–585: 1040–1055.

Haddad S, Paolini R, Ulpiani G, et al. (2020). Holistic approach to assess co-benefits of local climate mitigation in a hot humid region of Australia. *Scientific Reports*, 10: 14216.

Hellings A, Rienow A (2021). Mapping land surface temperature developments in functional urban areas across Europe. *Remote Sensing*, 13: 2111.

Iacono MJ, Delamere JS, Mlawer EJ, et al. (2008). Radiative forcing by long-lived greenhouse gases: Calculations with the AER radiative transfer models. *Journal of Geophysical Research: Atmospheres*, 113: D13103.

Imran HM, Kala J, Ng AW, et al. (2019). Impacts of future urban expansion on urban heat island effects during heatwave events in the city of Melbourne in southeast Australia. *Quarterly Journal of the Royal Meteorological Society*, 145: 2586-2602.

Jacob DJ, Winner DA (2009). Effect of climate change on air quality. *Atmospheric Environment*, 43: 51–63.

Jacobs SJ, Gallant AJE, Tapper NJ, et al. (2018). Use of cool roofs and vegetation to mitigate urban heat and improve human thermal stress in Melbourne, Australia. *Journal of Applied Meteorology and Climatology*, 57: 1747–1764.

Janjić ZI (1994). The step-mountain eta coordinate model: Further developments of the convection, viscous sublayer, and turbulence closure schemes. *Monthly Weather Review*, 122: 927–945.

Johnson H, Kovats S, McGregor G, et al. (2004). The impact of the 2003 heat wave on mortality and hospital admissions in England. *Epidemiology*, 15: S126.

Khan HS, Paolini R, Caccetta P, et al. (2022a). On the combined impact of local, regional, and global climatic changes on the urban energy performance and indoor thermal comfort—The energy potential of adaptation measures. *Energy and Buildings*, 267: 112152.

Khan A, Papazoglou EG, Cartalis C, et al. (2022b). On the mitigation potential and urban climate impact of increased green infrastructures in a coastal Mediterranean city. *Building and Environment*, 221: 109264.

Kolokotsa DD, Giannariakis G, Gobakis K, et al. (2018). Cool roofs and cool pavements application in Acharnes, Greece. *Sustainable Cities and Society*, 37: 466–474.

Kusaka H, Kondo H, Kikegawa Y, et al. (2001). A simple single-layer urban canopy model for atmospheric models: comparison with multi-layer and slab models. *Boundary-Layer Meteorology*, 101: 329–358.

Lai D, Liu W, Gan T, et al. (2019). A review of mitigating strategies to improve the thermal environment and thermal comfort in urban outdoor spaces. *Science of the Total Environment*, 661: 337–353.

Li D, Bou-Zeid E (2014). Quality and sensitivity of high-resolution numerical simulation of urban heat islands. *Environmental Research Letters*, 9: 055001.

Loughner CP, Allen DJ, Zhang D, et al. (2012). Roles of urban tree canopy and buildings in urban heat island effects: Parameterization and preliminary results. *Journal of Applied Meteorology and Climatology*, 51: 1775–1793.

McPhillips LE, Matsler AM (2018). Temporal evolution of green stormwater infrastructure strategies in three US cities. *Frontiers in Built Environment*, 4: 26.

Mellor GL, Yamada T (1974). A hierarchy of turbulence closure models for planetary boundary layers. *Journal of the Atmospheric Sciences*, 31: 1791–1806.

Middel A, Häb K, Brazel AJ, et al. (2014). Impact of urban form and design on mid-afternoon microclimate in Phoenix Local Climate Zones. *Landscape and Urban Planning*, 122: 16–28.

Mohammed A, Pignatta G, Topriska E, et al. (2020). Canopy urban heat island and its association with climate conditions in Dubai, UAE. *Climate*, 8: 81.

Mohammed A, Khan A, Santamouris M (2021). On the mitigation potential and climatic impact of modified urban albedo on a subtropical desert City. *Building and Environment*, 206: 108276.

Pyrgou A, Hadjinicolaou P, Santamouris M (2018). Enhanced near-surface ozone under heatwave conditions in a Mediterranean island. *Scientific Reports*, 8: 9191.

Qi J, Ding L, Lim S (2021). Toward cool cities and communities: A sensitivity analysis method to identify the key planning and design variables for urban heat mitigation techniques. *Sustainable Cities and Society*, 75: 103377.

Radhi H (2010). On the effect of global warming and the UAE built environment. In: Harris SA (Ed.), Global Warming. Rijeka, Croatia: InTech.

Santamouris M, Synnefa A, Karlessi T (2011). Using advanced cool materials in the urban built environment to mitigate heat Islands and improve thermal comfort conditions. *Solar Energy*, 85: 3085–3102.

Santamouris M (2014). Cooling the cities—A review of reflective and green roof mitigation technologies to fight heat island and improve comfort in urban environments. *Solar Energy*, 103: 682–703.

Santamouris M (2015a). Analyzing the heat island magnitude and characteristics in one hundred Asian and Australian cities and regions. *Science of the Total Environment*, 512–513: 582–598.

Santamouris M (2015b). Regulating the damaged thermostat of the cities—Status, impacts and mitigation challenges. *Energy and Buildings*, 91: 43–56.

Santamouris M, Ding L, Fiorito F, et al. (2017). Passive and active cooling for the outdoor built environment—Analysis and assessment of the cooling potential of mitigation technologies using performance data from 220 large scale projects. *Solar Energy*, 154: 14–33.

Santamouris M, Ban-Weiss G, Osmond P, et al. (2018). Progress in urban greenery mitigation science—Assessment methodologies advanced technologies and impact on cities. *Journal Civil Engineering and Management*, 24: 638–671.

Santamouris M (2020). Recent progress on urban overheating and heat island research. Integrated assessment of the energy, environmental, vulnerability and health impact. Synergies with the global climate change. *Energy and Buildings*, 207: 109482.

Santamouris M, Osmond P (2020). Increasing green infrastructure in cities: impact on ambient temperature, air quality and heat-related mortality and morbidity. *Buildings*, 10: 233.

Santamouris M, Yun GY (2020). Recent development and research priorities on cool and super cool materials to mitigate urban heat island. *Renewable Energy*, 161: 792–807.

Santamouris M, Paolini R, Haddad S, et al. (2020). Heat mitigation technologies can improve sustainability in cities. An holistic experimental and numerical impact assessment of urban overheating and related heat mitigation strategies on energy consumption, indoor comfort, vulnerability and heat-related mortality and morbidity in cities. *Energy and Buildings*, 217: 110002.

Sharma A, Fernando HJS, Hamlet AF, et al. (2017). Urban meteorological modeling using WRF: A sensitivity study. *International Journal of Climatology*, 37: 1885–1900.

Shashua-Bar L, Hoffman ME (2000). Vegetation as a climatic component in the design of an urban street: an empirical model for predicting the cooling effect of urban green areas with trees. *Energy and Buildings*, 31: 221–235.

Skamarock WC, Klemp JB, Dudhia J, et al. (2008). A description of the Advanced Research WRF Version 3. (No. NCAR/TN-475+STR)

Spahr KM (2020). Contextualizing and Communicating the Ancillary Benefits of Green Stormwater Infrastructure. PhD Thesis, Colorado School of Mines, USA.

Stathopoulou E, Mihalakakou G, Santamouris M, et al. (2008). On the impact of temperature on tropospheric ozone concentration levels in urban environments. *Journal of Earth System Science*, 117: 227–236.

Taleb H (2016). Effect of adding vegetation and applying a plants buffer on urban community in Dubai. *Spaces and Flows*, 7: 37–49.

Thompson G, Field PR, Rasmussen RM, et al. (2008). Explicit forecasts of winter precipitation using an improved bulk microphysics scheme. Part II: implementation of a new snow parameterization. *Monthly Weather Review*, 136: 5095–5115.

Tiedtke M (1989). A comprehensive mass flux scheme for cumulus parameterization in large-scale models. *Monthly Weather Review*, 117: 1779–1800.

Wang Y, Shen L, Wu S, et al. (2013). Sensitivity of surface ozone over China to 2000-2050 global changes of climate and emissions. *Atmospheric Environment*, 75: 374–382.

weatherspark (2022). Average Weather at Dubai International Airport United Arab Emirates. Available at https://weatherspark.com/y/148889/Average-Weather-at-Dubai-International-Airport-United-Arab-Emirates-Year-Round#Figures-WindSpeed

Wise EK (2009). Climate-based sensitivity of air quality to climate change scenarios for the southwestern United States. *International Journal of Climatology*, 29: 87–97.

Wong NH, Tan C, Kolokotsa DD, et al. (2021). Greenery as a mitigation and adaptation strategy to urban heat. *Nature Reviews Earth & Environment*, 2: 166–181.

Yu C, Hien WN (2006). Thermal benefits of city parks. *Energy and Buildings*, 38: 105–120.

Zhang C, Wang Y, Hamilton K (2011). Improved representation of boundary layer clouds over the southeast Pacific in ARW-WRF using a modified tiedtke cumulus parameterization scheme. *Monthly Weather Review*, 139: 3489–3513.

Zoulia I, Santamouris M, Dimoudi A (2009). Monitoring the effect of urban green areas on the heat island in Athens. *Environmental Monitoring and Assessment*, 156: 275–292.